223
12-9-81

(2)

I-293

14. 128

ORNL-5830

ornl

OAK RIDGE NATIONAL LABORATORY

UNION CARBIDE

MASTER

Radiation Facilities for Fusion-Reactor First-Wall and Blanket Structural-Materials Development

R. L. Klueh
E. E. Bloom

OPERATED BY
UNION CARBIDE CORPORATION
FOR THE UNITED STATES
DEPARTMENT OF ENERGY

ORNL-5830
Distribution
Category UC-20,20c

Contract No. W-7405-eng-26

METALS AND CERAMICS DIVISION

RADIATION FACILITIES FOR FUSION-REACTOR FIRST-WALL AND BLANKET STRUCTURAL-MATERIALS DEVELOPMENT

R. L. KLUEH and E. E. BLOOM

Date Published: December 1981

Paper presented at

Seminar on "Radiation Behavior of Materials

and Its Impact on Fusion Reactor Design"

Paris, France, August 25–26, 1981

OAK RIDGE NATIONAL LABORATORY
Oak Ridge, Tennessee 37830
operated by
UNION CARBIDE CORPORATION
for the
U.S. DEPARTMENT OF ENERGY

CONTENTS

RADIATION FACILITIES FOR FUSION REACTOR FIRST WALL AND BLANKET STRUCTURAL MATERIALS DEVELOPMENT

R. L. KLUEH and E. E. BLOOM

ABSTRACT

Present and future irradiation facilities for the study of fusion reactor irradiation damage are reviewed. Present studies are centered on irradiation in accelerator-based neutron sources, fast- and mixed-spectrum fission reactors, and ion accelerators. The accelerator-based neutron sources are used to demonstrate damage equivalence between high-energy neutrons and fission reactor neutrons. Once equivalence is demonstrated, the large volume of test space available in fission reactors can be used to study displacement damage, and in some instances, the effects of high-helium concentrations and the interaction of displacement damage and helium on properties. Ion bombardment can be used to study the mechanisms of damage evolution and the interaction of displacement damage and helium. These techniques are reviewed, and typical results obtained from such studies are examined. Finally, future techniques and facilities for developing damage levels that more closely approach those expected in an operating fusion reactor are discussed.

---

1. INTRODUCTION

Before fusion power reactors become a reality, many technological problems must be solved. One of the most important involves the choice of materials for first wall and blanket structures. The lifetime of these structural components will have a major effect on the economic viability of fusion energy.

During service the first wall and blanket structures will operate at elevated temperatures in a corrosive environment (e.g., Li, Li_2O Li_7Pb_2) within a strong neutron radiation field. Many reactor designs call for pulsed operation, which then leads to cyclic stresses, temperatures, and neutron fluxes. Because of the range of contemplated operating conditions for proposed fusion reactor designs, several alloy systems have been considered for the first wall and blanket structures. These include the high-strength Fe-Ni-Cr superalloys and alloys based

on niobium, vanadium, and titanium, as well as more conventional alloys such as austenitic stainless steel (e.g., type 316) and chromium-molybdenum ferritic (martensitic) steels. Austenitic stainless steels are presently seen as the material most likely to be used for first-generation reactors.

It is the exposure of the first-wall and blanket structures to unique radiation conditions that has caused the materials specialists the most concern. In the extensive testing programs that preceded the development of thermal and fast fission power reactors, prototypic test reactors were available well in advance of the construction of the first demonstration power reactors. No such prototype reactor is presently available for the fusion program, and none will be available until the 1990s (a demonstration reactor is planned for early in the twenty-first century). Thus, the challenge is to use existing facilities to develop and qualify materials for the first fusion reactors that produce significant power. To do this, the irradiation effects that are expected to be produced by the intense high-energy neutron flux generated in an operating fusion reactor must be "simulated." These simulations must be carried out by irradiating materials in existing fission facilities or by irradiating with other techniques (e.g., ion irradiation) that allow for the generation of damage similar to that expected in a fusion reactor. Because all facilities short of a fusion reactor have significant shortcomings, it will also be necessary to develop an understanding of radiation-damage mechanisms so that the effects developed during simulation can be correlated with those formed in a fusion reactor environment.

2. IRRADIATION DAMAGE IN A FUSION REACTOR

For at least the first generation fusion reactors, energy will be derived from the deuterium-tritium (D-T) fuel cycle through the following fusion reaction:

$$D + T \rightarrow He + n + \text{energy} . \qquad (1)$$

Approximately 17.6 MeV of energy results, 3.5 MeV as kinetic energy of the alpha particle (helium) and 14.1 MeV as kinetic energy of the neutron. Most of the energy from the helium is deposited in the plasma and transferred by electromagnetic and charged-particle radiation to surfaces facing the plasma. Although this may give rise to materials problems, due mainly to high heat loads, they will not be discussed in this paper. It is the disposition of the remaining energy (~80%) carried by the high-energy neutron that causes the irradiation effects that are the subject of this paper.

Irradiation damage studies of metals and alloys exposed to fission reactor neutrons have demonstrated a considerable effect on physical and mechanical properties; the most important effects involve the loss of ductility and the swelling of the irradiated material. The objective of the irradiation-effects studies under fusion reactor conditions is the determination of the effect on the properties of potential structural materials.

The primary difference between the fusion reactor irradiation environment and that in the core of a fission reactor is the high-energy component of the neutron spectrum (up to 14.1 MeV) resulting from the fusion reaction (Fig. 1). (The average creation energy of neutrons in a fast reactor is about 2 MeV.) The high energy of the neutrons in a fusion reactor environment gives rise to larger amounts of displacement damage per neutron interaction with a lattice atom. Displacement implies the displacement of an atom from its normal lattice position and is initiated by the collision of a neutron with a lattice atom, which results in a vacancy (vacant lattice site) and an interstitial atom. When the displaced atom has sufficient energy it can displace other lattice atoms. The extent of the displacement damage is expressed in terms of how often an atom is displaced from its normal lattice position as displacements per atom, or dpa.

In addition to the displacement damage, neutrons in both fission and fusion reactors give rise to transmutation reactions. These reactions produce solid products and helium and hydrogen gas within the structural materials. Some solid transmutation products of interest that have been considered include manganese, vanadium, and titanium in

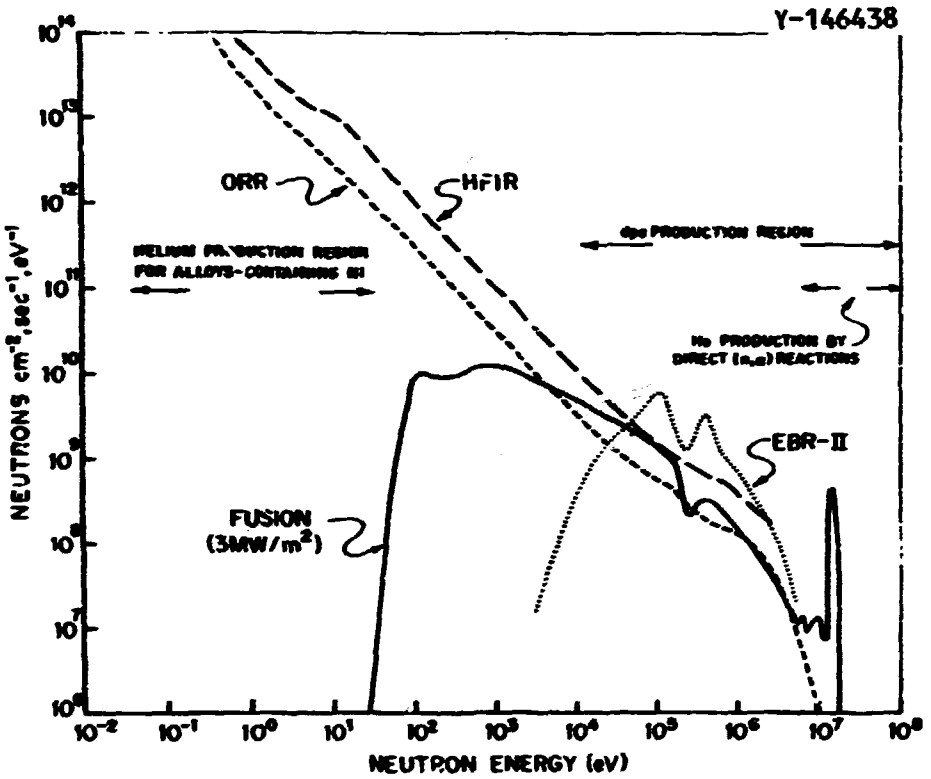

Fig. 1. Neutron-energy spectra for various fission reactors and the spectrum at the first wall of a lithium-cooled fusion reactor. The primary difference between the spectra of the fission and fusion reactors occurs above 10^7 eV.

austenitic stainless steels and silicon in aluminum [1]. In a recent review, Wiffen and Stiegler concluded that at present there are no indications of a detrimental effect of solid transformation products on properties [1]. It is also generally felt that hydrogen will have little effect on the properties of fusion reactor components [1,2]. At the operating temperatures of fusion reactors (250–550°C), the hydrogen should readily diffuse from the structures. Although some ion-irradiation studies have indicated that preinjected hydrogen may have an effect on cavity nucleation [3,4], studies where hydrogen and helium were injected simultaneously with nickel ions indicated little effect of hydrogen [5]. Solid transmutation products and transmutation hydrogen will not be further discussed in this paper.

From fission reactor radiation-damage studies, it is known that small amounts of transmutation helium produced within the lattice can have pronounced effects on properties [6,7]. Helium is essentially

insoluble in metals and alloys. As a result, the helium atom affects void nucleation and swelling; at elevated temperatures the collection of helium gas on grain boundaries leads to a loss of ductility — helium embrittlement. In Fig. 2 the cross section for the (n,α) reactions for iron, nickel, and chromium are shown as a function of neutron energy. As a result of the high cross section at neutron energies corresponding to those present in the fusion spectrum, much larger concentrations of transmutation helium are produced by a fusion reactor neutron spectrum than by a fast fission reactor (Table 1). The evolution of the microstructure during irradiation depends in large measure on the interaction of the helium with the displacement damage. For that reason it is important that irradiation damage studies take proper account of the helium production rates that are appropriate for an operating reactor.

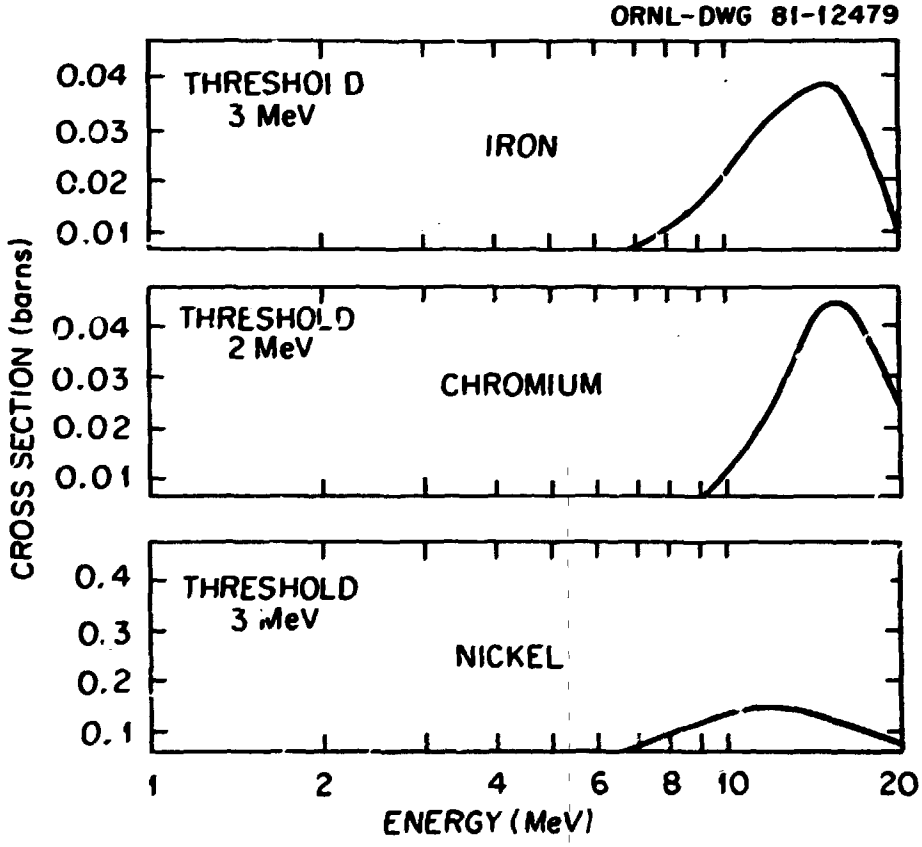

Fig. 2. Cross section for (n,α) reactions for iron, chromium, and nickel as a function of neutron energy.

Table 1. Atom-Displacement Rates and Helium-Production Rates in Fusion and Fast-Fission (EBR-II) Reactor Spectra

Material	Fusion Reactor[a] at 1 MW/m^2		EBR-II (Row 2)	
	dpa/s 10^{-7}	at. ppm He/s 10^{-7}	dpa/s 10^{-7}	at. ppm He/s 10^{-7}
Type 316 stainless steel	3.6	47	10.0	6.1
Vanadium	3.6	15	12.0	0.4

[a]Many current conceptual designs call for neutronic wall loadings of 2–3 MW/m^2.

The economic viability of a fusion reactor will be strongly influenced by the length of time the structural materials can survive the reactor operating conditions. With this in mind and assuming that radiation damage will limit the life of the structural materials in the first wall and blanket structure, the United States Department of Energy Fusion Program initially chose the following criteria for evaluating structural materials: "A satisfactory material will survive an exposure equivalent to 40 MW·y/m^2 at a temperature which allows the reactor to operate with conventional liquid metal steam generators similar to those contemplated for use in breeder reactor systems" [8]. (The 40 MW·y/m^2 wall loading refers to the product of plasma neutron wall loading in megawatts per square meter and the lifetime in years; reactor designs call for plasma neutron wall loadings of 1–3 MW/m^2.) In recent years design studies have indicated that fusion reactors may be economical at integrated wall loading values less than half the 40 MW·y/m^2. Also, designs for water or helium heated steam generators have been considered. Regardless of the economic criteria, one of the objectives of any alloy development program will ultimately be the testing of materials to an equivalent reactor service time and beyond (20–40 MW·y/m^2).

The remainder of this report will be devoted to a review of the techniques and facilities that are presently being used to simulate, study, and understand the type of irradiation effects expected in the

first wall and blanket structures. We will review the types of results generated in existing irradiation facilities and the limitations of these facilities. Finally, we will examine the facilities and tests that will eventually allow for studies on materials at irradiation conditions that begin to approach the neutronic wall loadings expected in a fusion reactor.

3. IRRADIATION DAMAGE STUDIES IN EXISTING FACILITIES

An ideal irradiation test system should have a fusion neutron spectrum (Fig. 1), which would be peaked at 14.1 MeV with a neutron flux in the range 5×10^{17}–5×10^{18} neutrons/($m^2 \cdot s$). Such a facility should have a test volume of up to 10 liters to enable large numbers of test specimens (mechanical properties and microscopy specimens) to be irradiated simultaneously. Because no such facility exists, radiation damage studies must presently rely on existing fission reactors and other simulation techniques (e.g., accelerator-based neutron sources and ion accelerators) to understand the underlying processes that occur during irradiation. The results of these studies will then be used to extrapolate material behavior to fusion reactor conditions. Eventually, facilities are expected to become available that will allow the testing of materials at conditions comparable to those expected in a fusion reactor.

Fission reactors are the only available facilities that provide the large volume of test space required to develop improved radiation-resistant materials or to qualify materials for fusion reactor service. Before existing fission reactors can be used to simulate the radiation damage, however, the equivalence of the lattice damage caused by 14 MeV neutrons and neutrons of lower energy generated in a fission reactor needs to be established. Such studies have been conducted in accelerator based high-energy neutron sources. Because of the small irradiation volume and the low-flux gradients of such facilities, only limited numbers of small specimens can be irradiated. The low fluences of irradiations in accelerator-based high-energy neutron sources preclude the formation of significant amounts of helium.

Once damage equivalence is established, the larger test specimens needed to carry out mechanical properties studies must be irradiated in fission reactors. Fast-spectrum fission reactors can be used to simulate the displacement damage expected in a fusion reactor during its lifetime. However, in a fast reactor where the average neutron energy is less than 1 MeV, this displacement damage occurs without the buildup of the high concentrations of transmutation helium that occurs in a fusion reactor. Under certain conditions, helium can be generated in mixed-spectrum reactors in the amounts expected in a fusion reactor. It is also possible, under certain circumstances, to achieve He/dpa ratios similar to those expected in fusion reactors.

Ion bombardment offers another technique for studying the effect of helium and displacement damage. Heavy ion bombardment can be used to study displacement-damage effects, and with dual- or triple-beam techniques, simultaneous displacement damage and gas effects can be determined.

In this section these three types of irradiation facilities will be examined; the types of results that are obtained from each facility will also be discussed.

3.1 High-energy, accelerator-based neutron sources

The accelerator-based Rotating Target Neutron Source (RTNS-II) is the only available 14 MeV neutron source presently available to the fusion program. To generate the high-energy neutrons, deuterons are accelerated to 400 kV. A 150-mA beam of these deuterons strikes a rotating, water-cooled copper target; the target is coated with titanium tritide. The 14.1 MeV neutrons are produced by the T(d,n) reaction. When the deuteron beam is focused on a 1 cm^2 spot, the resulting neutron beam flux is ~1.3×10^{17} neutrons/($m^2 \cdot s$) [9,10]; the usable flux depends on the distance from the source (Fig. 3). The primary test space in the RTNS-II is about 2-cm thick by 10-cm diameter. Over this volume, the flux ranges from 1.3×10^{17} to 5×10^{15} neutrons/($m^2 \cdot s$) [9].

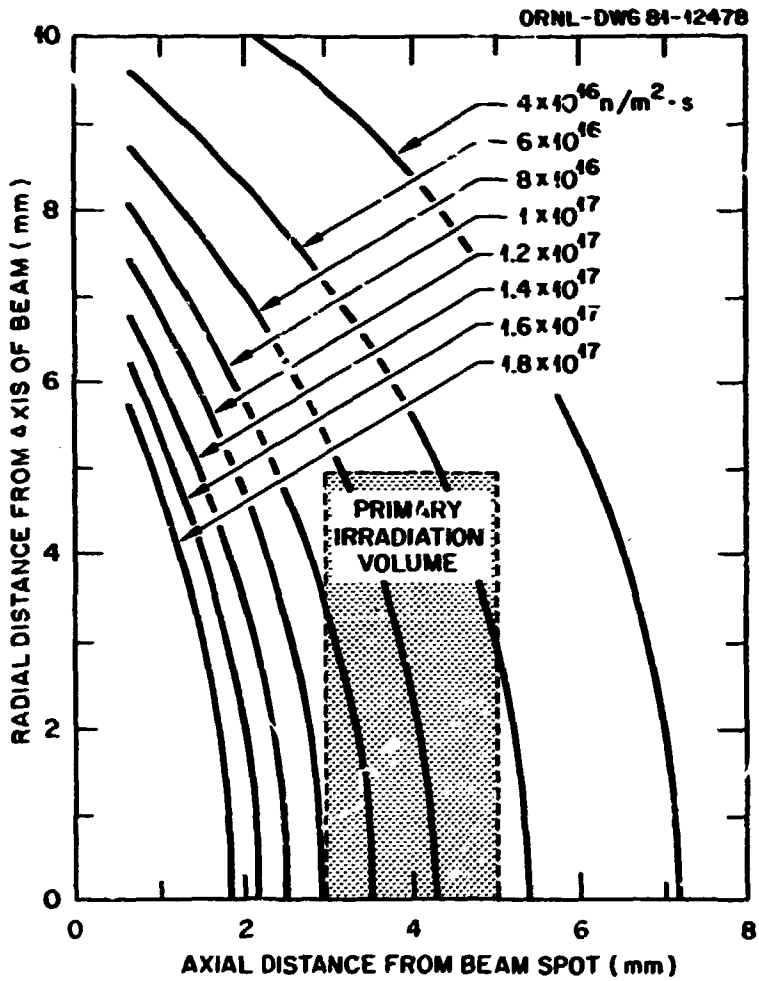

Fig. 3. Constant-flux contours of the neutron field of the RTNS-II source (taken from ref. [9]).

A second method for generating high-energy neutrons is the deuteron-beryllium (d-Be) source, in which an accelerated beam of 15–40 MeV deuterons is stopped by a beryllium target. The deuteron breakup reaction [Be(d,n)] then results in a neutron beam with a spectrum broadly peaked near 15 MeV, although it includes energies from thermal to 30 MeV [11–13]. As with the RTNS-II, the usable flux for such a source is quite low, in the range 2×10^{16}–1×10^{17} neutrons/($m^2 \cdot s$) ($E > 1$ MeV). Likewise, the test volume is small (less than that available in RTNS-II).

The RTNS-II and Be(d,n) sources have been used primarily to correlate the damage produced by high-energy neutrons with the damage produced by lower energy neutrons in fission reactors. Because of

the limited availability of high-energy neutron sources, most irradiations have been confined to ambient temperature, low fluences, and relatively pure metals such as gold, copper, niobium, vanadium, and molybdenum. Pure metals were chosen because they are sensitive to low fluences and are well understood from studies of low-energy neutron effects. Many of the early studies involved measurement of physical properties such as resistivity [1].

An energy transfer of a few tens of electron volts from a bombarding neutron to a lattice atom can lead to displacement damage: lattice atoms are removed from their normal lattice positions, resulting in the formation of vacancies and interstitials. The primary knock-on atom (PKA) that results from such a neutron collision can cause other displacement events as the energy of the PKA is dissipated. The maximum energy of a PKA depends on the energy of the bombarding particle. This could lead to the possibility that the damage produced by 14 MeV neutrons is substantially different from that of lower energy neutrons.

The work that has been completed to date shows excellent correlation between displacement damage produced by 14.1 MeV neutrons and that from other sources, thus providing confidence that the data derived from fission reactor studies are meaningful for fusion systems. This work has been reviewed by Wiffen and Stiegler [14].

For neutrons of several hundred keV, the PKA can transfer energy to surrounding atoms. Some of these atoms are displaced, and can, in turn, displace other atoms. The end result is a displacement cascade in the region around the path of the original PKA. A displacement cascade can be described in terms of the vacancies and interstitials created by the collision of the PKA and secondarily displaced atoms with other lattice atoms. Basically, the cascade consists of a vacancy-rich core or depleted zone that is surrounded by a diffuse shell of interstitial atoms. Experiment and theory show that when the energy of the PKA exceeds some threshold value, more than one cascade forms; these are called subcascades [14]. Thus, the differentiation of the damage by high-energy neutrons in a fusion reactor spectrum and those from a fission reactor involves the difference between the formation of subcascades and cascades.

The results of quantitative transmission electron microscopy studies that compared the damage caused by 14 MeV neutrons with lower energy neutrons revealed no unexpected damage structures for the high-energy neutrons [12–16]. Although there were differences in size and distribution of the damage, the nature of the damage was essentially the same. Damage at the low temperatures takes the form of small defect clusters or dislocation loops, regardless of the neutron energy. The loops result from either a collapse into clusters of vacancies and interstitials within the cascade or subcascade region, or from interstitials clustering in the matrix; uncollapsed regions cannot generally be observed [14].

In studies on gold foils, Merkle concluded that essentially any collision with an energy transfer that exceeds 50 keV will produce a dislocation loop that is visible by transmission electron microscopy [14]. Different energies are required for other metals and alloys. The net result of this work is an indication that there is no difference in the structure of cascades and subcascades. Furthermore, it appears that the amount of displacement produced by 14 MeV neutrons can be calculated within a factor of about 2 [1,12–14].

The dislocation loop structures produced in copper and niobium irradiated in a d-Be neutron source and a fission reactor were compared by Roberto, Narayan, and Saltmarsh [12]. Electron microscopy and x-ray scattering techniques were used to show that loop concentrations and sizes agreed closely for the two neutron spectra for irradiations to equivalent damage levels. Further work by Narayan and Ohr on niobium showed that the defect-cluster behavior was essentially independent of neutron energy [13]. When compared on a damage-energy basis, it was found that damage levels were similar for equivalent deposited damage energy. (Damage energy is defined as the fraction of the bombarding particle's energy that is available to produce displacements; it is closely related to dpa).

For most metals and alloys, cascades and subcascades are not directly visible by transmission electron microscopy; only the dislocation loops can be observed. Recently, however, English and Jenkins showed that zones of reduced long-range order formed at a cascade site in well

ordered Cu_3Au could be directly imaged by transmission electron microscopy [15]. In this alloy system, the investigators were able to obtain quantitative information on individual cascades. This work involved irradiation by 3.5 MeV protons, fission neutrons, and fusion neutrons from RTNS-II and was an elegant confirmation and extension of earlier work.

The initial studies on the effect of neutron energy on the room-temperature yield stress of niobium and copper by Mitchell et al. [16] indicated identical qualitative effects of 14 MeV neutron and fission reactor irradiation. The dislocation loop structure produced by both types of irradiations resulted in rapid strengthening after an apparent threshold fluence was passed. However, the strengthening versus fluence curves were displaced by a factor of 10-20 in strength and the rate of hardening per unit fluence was approximately ten times greater for the 14 MeV neutrons.

Recent work by Vandervoort et al. on annealed type 316 stainless steel has further quantified the relationship between 14 MeV neutrons and those from a fission reactor [17]. These investigators examined the effect of irradiation at 25°C by neutrons from the RTNS-II and a Be(d,n) source and at 60°C by neutrons from a fission reactor (Livermore Pool Type Reactor). They compared the damage produced by each source and determined the effect of the irradiation on yield strength and ductility. Like Mitchell et al. [16], they found that the 14 MeV neutron irradiation produced greater strengthening than the other two sources when compared on a fluence basis — that is, the curves were displaced [Fig. 4(a)]. When compared on a damage-energy basis, however, equivalent effects were noted [Fig. 4(b)]. Similar results were obtained for ductility and defect-cluster density (Fig. 5) when examined as a function of fluence and damage energy. The observations on defect density help explain the effect on the yield strength. That is, for equivalent fluences, the high-energy neutrons produced more defect clusters than fission neutrons, while the number of defect clusters for a given damage energy are essentially the same for the neutrons produced in the three sources [17].

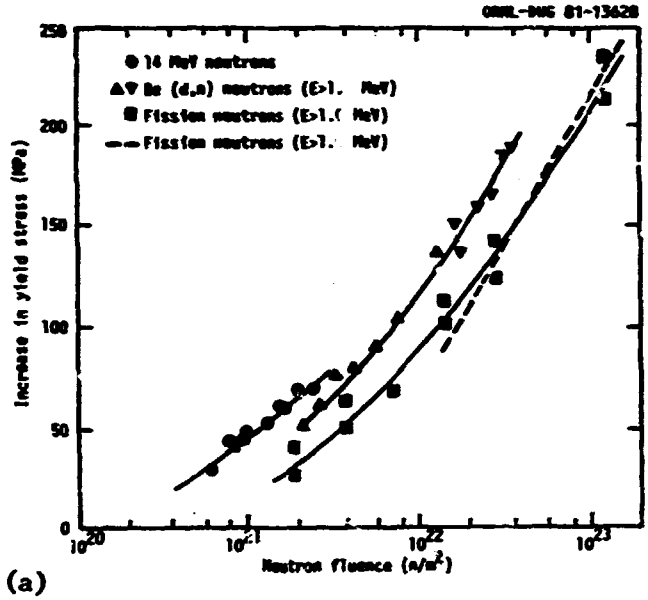

(a)

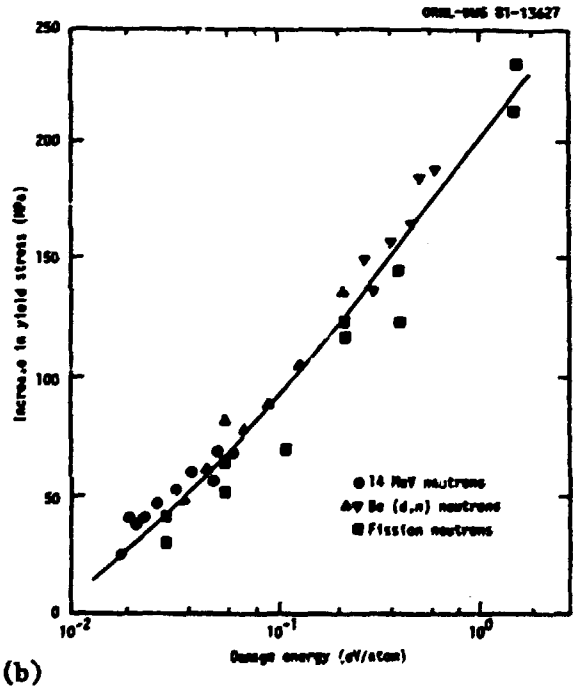

(b)

Fig. 4. Radiation strengthening of type 316 stainless steel. (a) As a function of neutron fluence, and (b) as a function of damage energy. Taken from ref. [17].

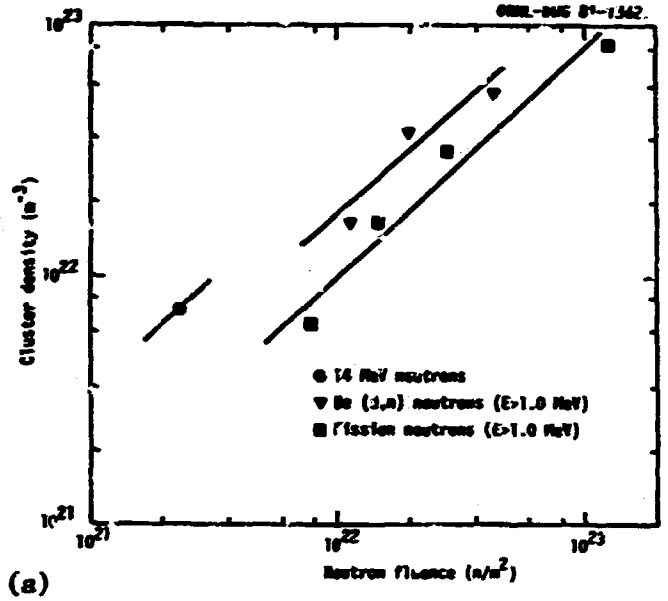

(a)

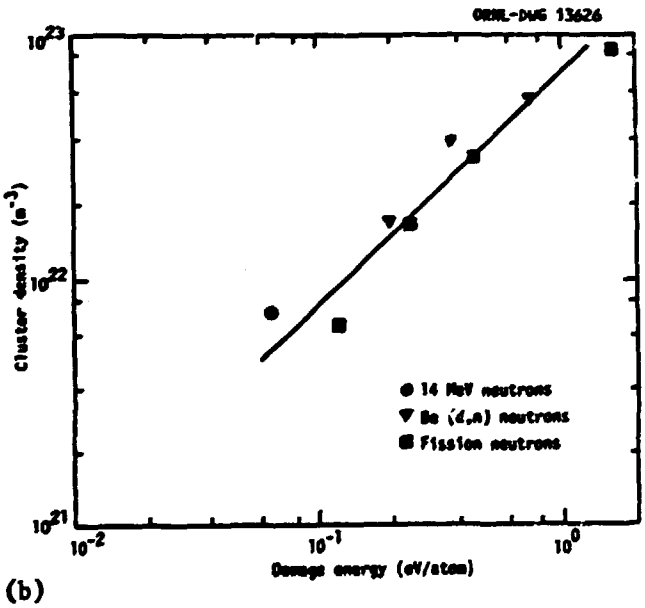

(b)

Fig. 5. Density of radiation-induced defects in type 316 stainless steel. (a) As a function of neutron fluence, and (b) as a function of damage energy. Taken from ref. [17].

Work continues on RTNS-II to further refine our understanding of the damage processes and the effect of high-energy neutrons on physical and mechanical properties. Data have also been obtained from an in situ neutron-induced creep test on niobium at 550 and 600°C [18]. Further tensile, microhardness, transmission electron microscopy and in situ resistivity measurements on various alloys are in progress.

3.2 Fission reactors for fusion reactor simulation

The studies using the accelerator-based high-energy neutron sources have demonstrated the equivalence of displacement damage (equivalence in type, form, and amount) by 14 MeV neutrons and neutrons from fission reactors when correlated on a damage-energy basis. Because the evolution of the irradiated structure proceeds from the cascade structure, these studies demonstrated the feasibility of using fast-reactor irradiation to study the effect of displacement damage on mechanical properties and swelling. In addition to the displacement damage, the high-energy neutrons in a fusion-reactor spectrum generate helium by (n,α) transmutation reactions in essentially all constituents of the contemplated first-wall and blanket-structure alloys [19]. The amounts of helium generated are proportional to the cross sections of the various elements. Because of the low-flux limitations of the presently available high-energy neutron sources (RTNS-II and d-Be), it is not possible to produce the large amounts of helium typical of first-wall structures under fusion-reactor conditions. Thus, other techniques must be used to generate radiation damage data at He/dpa ratios expected for fusion reactors. For certain alloys, mixed-spectrum fission reactors are appropriate for such studies.

3.2.1 Fast reactors

In the Experimental Breeder Reactor (EBR-II), test materials are irradiated in uninstrumented capsules (~19-mm diameter × 330-mm long) with temperature controlled by variable-thickness gas gaps or in some instances by heat pipes [10]. The peak fast flux of EBR-II is about 3×10^{19} neutrons/($m^2 \cdot s$) ($E > 0.1$ MeV) with a mean neutron energy of

~0.85 MeV. This results in a displacement damage rate of 10–20 dpa/y in stainless steel, an exposure equivalent to 0.8–1.8 MW·y/m^2 in a fusion reactor. However, only about 10–40 at. ppm He are generated, an equivalence of 0.06–0.12 MW·y/m^2. It is possible to study helium effects in fast reactors using preinjected specimens. Because of the uncertain value of this technique, the EBR-II is used primarily to study the effects of high displacement damage on alloys of interest and other methods are used to study helium effects.

In the near future (1982), the Fast Flux Test Facility (FFTF) will offer another fast-spectrum irradiation facility for fusion-simulation studies. The FFTF will have a higher flux and larger test volume than EBR-II, and it will offer the possibility of conducting instrumented tests. For the test space in Row 4 of FFTF, the flux is ~6 × 10^{19} neutrons/(m^2·s) with average energy ~0.45 MeV. This results in a damage rate of 40–60 dpa/y, the equivalent of 4–6 MW·y/m^2. At such a flux it will be possible to produce the displacement damage expected for 40 MW·y/m^2 in about ten years. However, this would again occur with a small helium-generation rate relative to that for a fusion reactor.

Both EBR-II and FFTF have a lower irradiation temperature limitation of approximately 370°C. This temperature is determined by the reactor coolant inlet temperature. Because operating temperatures for several reactor designs are below this temperature, irradiation test capabilities at lower temperatures are required.

3.2.2 Mixed-spectrum reactors

Although fast reactors offer the possibility of irradiating materials to damage levels similar to those achieved in a fusion reactor, it is not possible to simultaneously generate the transmutation helium that will form in alloys exposed to a fusion-reactor neutron spectrum. However, for alloys that contain nickel, mixed-spectrum reactors can be used to simulate the effect of simultaneous displacement damage and transmutation helium formation.

This simulation relies on a different transmutation reaction from the one-step (n,α) reaction with high-energy neutrons that yields the helium

during fusion-reactor service. Nickel undergoes the following two-step helium transmutation reaction with thermal neutrons:

$$^{58}Ni + n \rightarrow {}^{59}Ni + \gamma \quad ; \tag{2}$$

$$^{59}Ni + n \rightarrow {}^{56}Fe + {}^{4}He \quad . \tag{3}$$

This reaction sequence is of importance for nickel-bearing alloys irradiated in mixed-spectrum reactors such as the Oak Ridge Research Reactor (ORR) or the High Flux Isotope Reactor (HFIR), where the spectra have both thermal and fast neutrons.

In Fig. 1 the region of the neutron-energy spectrum where reactions (2) and (3) occur is indicated. The relationship of the neutron-energy spectra of ORR, HFIR, and EBR-II to a fusion reactor spectrum can also be seen. Table 2 shows a comparison of the displacement damage and helium production after one year for type 316 stainless steel in a fusion reactor first wall (1 MW/m^2) as compared to those of EBR-II, ORR, and HFIR, the three reactors that have been used most extensively for fusion reactor studies.

The ORR is being used extensively to irradiate austenitic stainless steels and nickel alloys where helium is generated according to reactions

Table 2. Atom Displacements and Helium and Hydrogen Production in Type 316 Stainless Steel After One Year's Operation[a]

Reactor[b]	Neutron Fluence (neutrons/m^2) (>0.1 MeV)	Displacements (dpa)	Helium (at. ppm)	Hydrogen (at. ppm)
Fusion reactor (1 MW/m^2)	0.80×10^{26}	11.5	144	530
EBR-II	6.9×10^{26}	37	~20	300
HFIR	4.4×10^{26}	35	1900[c,d]	425
ORR	1.3×10^{26}	11	80 to 160	135

[a]Taken from F. W. Wiffen et al., Metal Science of Stainless Steel, AIME, New York, 1978, p. 146.
[b]A high-flux position has been chosen for each reactor, and a duty fraction of 1.0 has been assumed. Abbreviated reactor designations are explained in text.
[c]Measured value.
[d]These values are not linear in time.

(2) and (3). The ORR has six prime positions where instrumented capsules 60 mm × 60 mm × 0.61-m length can be inserted. The reactor has peak fast and thermal fluxes of 3×10^{18} (E > 0.1 MeV) and 2.4×10^{18} neutrons/(m^2-s), respectively. For type 316 stainless steel this results in ~12 dpa and 120 at. ppm He per year, a first-wall exposure equivalent to 0.9 and 0.7 MW·y/m^2, respectively.

The HFIR has respective peak fast and thermal neutron fluxes of 1.5×10^{19} (E > 0.1 MeV) and 2.4×10^{19} neutrons/(m^2·s) which in one year will generate 34 dpa and 1900 at. ppm He in type 316 stainless steel, corresponding to ~2.6 and 10.7 MW·y/m^2. The space in the six water-cooled peripheral target positions is 18-mm dia × 0.6-m long. Numerous other high-flux positions are also available. No instrumentation is presently possible in the highest flux regions of HFIR.

For a fusion reactor first-wall structure, displacement damage and helium concentration are linearly related (Fig. 6). In the ORR or HFIR, the ratio of thermal-to-fast neutrons remains approximately constant during the irradiation. For a thermal flux ϕ_t, the transmutation helium

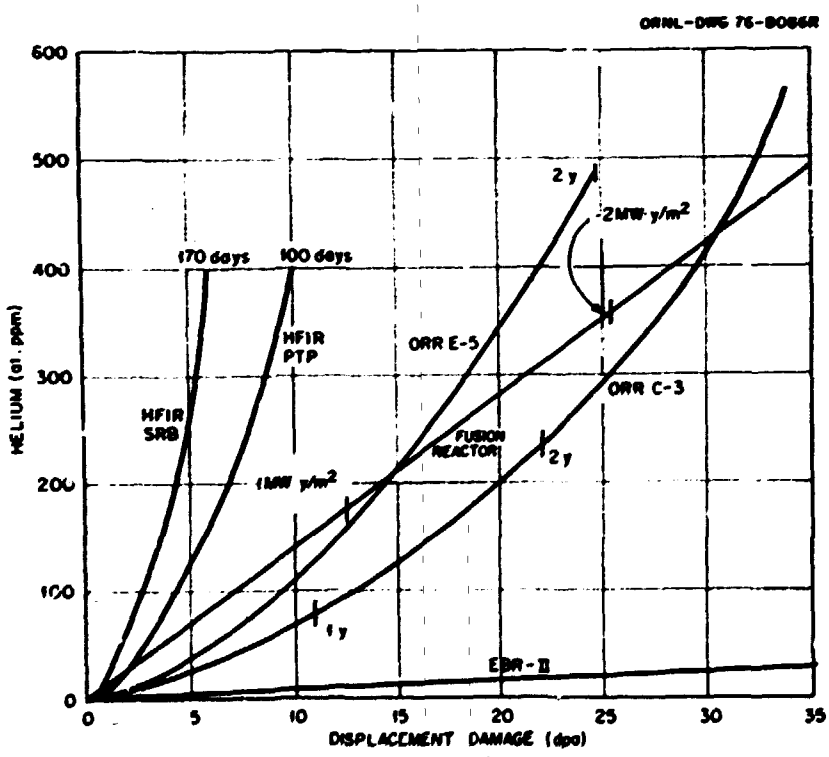

Fig. 6. Helium concentration as a function of displacements per atom for type 316 stainless steel for a fusion reactor first wall and for irradiation in two positions each of HFIR and ORR. Various time intervals at full power are shown.

that forms by reactions (2) and (3) increases with time t as $(\phi_t t)^n$ (n depends on irradiation time and decreases from ~2 to 1.4 during irradiation). The displacement damage (dpa) depends on the fast flux ϕ_f and increases as $\phi_f t$. Thus, a He/dpa ratio similar to that achieved in a fusion reactor occurs at only one time when the nickel-containing alloy is irradiated (Fig. 6). For comparison, the He-dpa relationship for EBR-II is also shown in Fig. 6.

This discussion demonstrates that it is possible to use presently available fission reactors to irradiate and study materials that have displacement damage (EBR-II and FFTF) and helium concentrations (ORR and HFIR) similar to those produced in a fusion reactor first wall. The problem is to achieve simultaneous production of helium and displacement damage at ratios similar to those produced in a fusion reactor. Before we discuss this problem, however, we will first examine results that have been obtained using fission reactors under normal operating conditions.

3.2.3 Materials studies in fission reactors

Although fission reactor irradiations do not allow for the study of radiation damage effects under prototypic fusion reactor conditions, most of the information relative to material behavior under these conditions has been obtained from studies using fission reactors. A substantial amount of work has been done in the Fast Breeder Reactor (FBR) program to determine the effect of fast-spectrum irradiation on candidate fuel-cladding alloys. In the United States, most work was on austenitic stainless steels, and in particular, type 316. Cold-worked type 316 stainless steel has been chosen as the fuel cladding for the demonstration LMFBR. Because of the large amounts of data already available for type 316 stainless steel, this alloy became the focal point when radiation damage studies began on first-wall and blanket-structure alloys [20].

The effect of fast-reactor (EBR-II) irradiation on the austenitic stainless steels has been reviewed [6,21–23]. Changes occur in strength, deformation, fracture behavior, and ductility. These changes can be directly related to the microstructural changes caused by the displacement damage during irradiation and the small amount of transmutation helium

produced. Another important property change is that of swelling due to void formation, which results in a volume increase, ΔV, and is reported as $\Delta V/V$ in percent. Swelling results when vacancies and interstitials are accepted by different sinks; volume increases of several tens of percent are observed in stainless steel.

For irradiation temperatures $T_I < 0.35\ T_m$ (~350°C in stainless steel), where T_m is the absolute melting temperature, irradiation-produced dislocation loops that result from the clustering of interstitials and/or vacancies formed during irradiation cause an increase in flow stress and a decrease in uniform elongation. At high damage levels, a change may occur in the deformation mode, from homogeneous to planar or channel deformation [6]. Between $0.35\ T_m < T_I < 0.6\ T_m$ (~350–700°C in stainless steel), a void and dislocation structure forms to produce swelling. The effects on tensile flow properties are similar to those at the low temperatures, while creep fractures become intergranular. Finally, at $T > 0.6\ T_m$ (~700°C in stainless steel), displacement damage is no longer stable; flow properties are unaffected by irradiation. However, the ductility decreases because of helium embrittlement. This occurs even for the low helium concentrations developed in fast reactors (Table 1).

In the fusion reactor program, considerable effort has been directed at determining the effect of helium on irradiated properties. Much of this work has involved the irradiation of type 316 stainless steel in mixed-spectrum reactors (where large amounts of helium and displacement damage are generated) and comparing the results with those obtained from fast-reactor (i.e., EBR-II) irradiation (where large amounts of displacement damage occur). Note that the displacement damage in HFIR is similar to that of EBR-II (Table 2).

The first comparative swelling results obtained from EBR-II and HFIR are shown in Fig. 7. These results show the difference in the swelling behavior of solution-annealed and cold-worked type 316 stainless steel irradiated in the two reactors. The cold-worked steel showed considerably less swelling than the solution-annealed steel in both the EBR-II and HFIR. At the highest temperatures, recrystallization and grain growth in the cold-worked steel causes it to lose its low-temperature advantage.

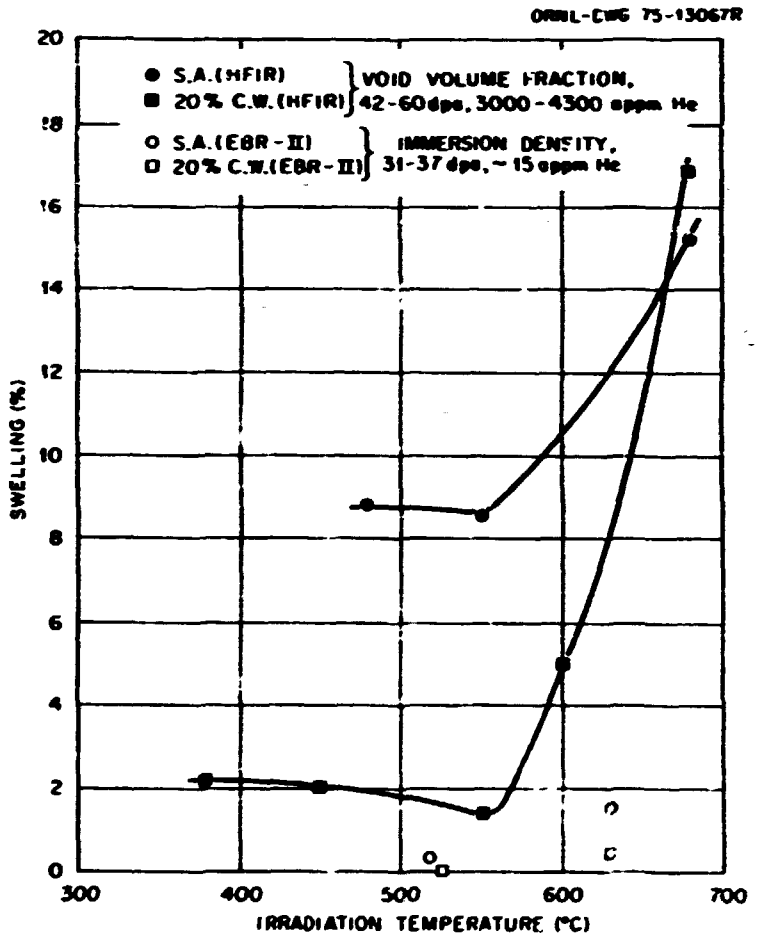

Swelling vs Temperature

Fig. 7. Effect of helium and cold work on the swelling of type 316 stainless steel in HFIR and EBR-II.

The history of the ongoing interpretation of the helium-effects studies is interesting because it shows the difficulties involved in such studies. Initially, the much greater swelling indicated for the HFIR-irradiated steel (Fig. 7) was attributed to the larger helium concentrations (3000–4300 at. ppm for HFIR, ~15 at. ppm for EBR-II) [24]. Because the HFIR-irradiated material in Fig. 7 was at a higher displacement damage level than the EBR-II-irradiated steel, as more data became available the swelling data were re-examined in terms of dpa at a given temperature (500°C) [Fig. 8(a)]. From these results it appeared that helium played a minor role in the swelling process in 20%-cold-worked type 316 stainless steel [25].

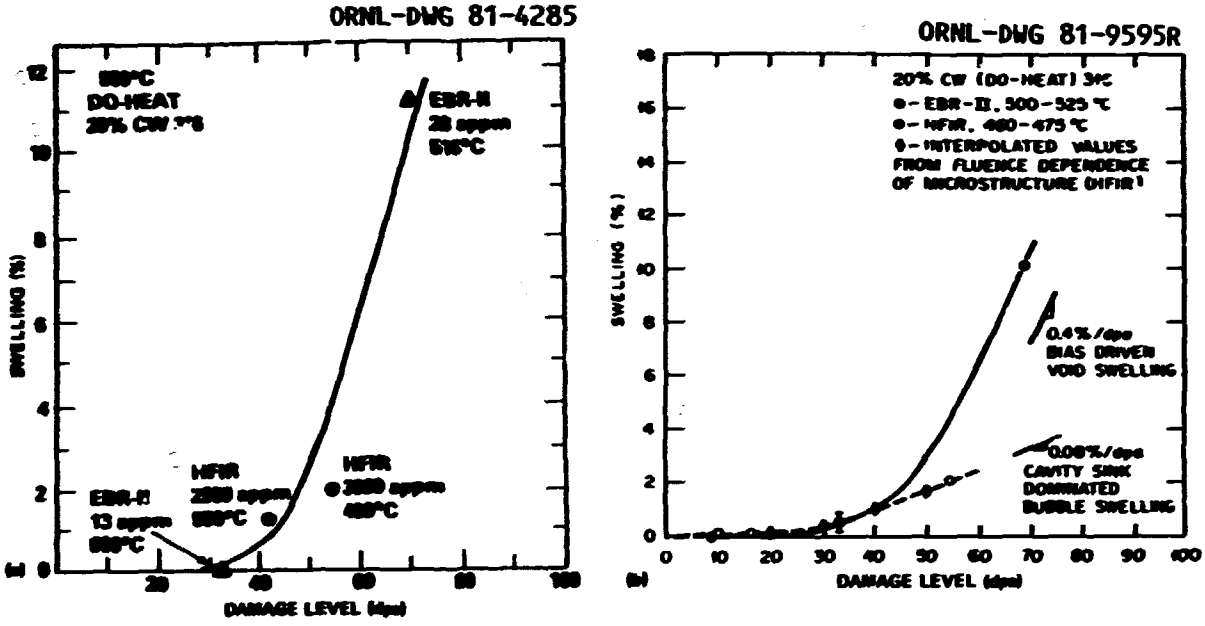

Fig. 8. Swelling as a function of fluence for 20%-cold-worked type 316 stainless steel irradiated in EBR-II and HFIR at ~500°C. (a) Data are interpreted as if helium has no effect on swelling [25]. (b) Data interpreted in terms of cavity growth mechanisms that indicate a helium effect [26].

More recently, Maziasz has examined a large number of TEM specimens of 20%-cold-worked type 316 stainless steel irradiated to similar dpa levels in both HFIR and EBR-II [26]. These results indicate that at 500°C helium not only affects the swelling behavior [Fig. 8(b)], it also affects the precipitation process. At low dpa for EBR-II-irradiated specimens, scattered cavities develop on dislocations and precipitates [Fig. 9(a)]. In HFIR-irradiated specimens, a high density of uniformly distributed matrix cavities form, along with cavities on precipitates [Fig. 9(b)]. This difference is accompanied by an increased precipitation rate and slightly increased swelling rate in the HFIR-irradiated specimens. At higher fluences a similar difference in cavity microstructure was observed, but the swelling rate was considerably greater in EBR-II irradiated specimens [Fig. 10]. However, similar precipitates were now present in both specimens. In Fig. 8(b) it is found that the swelling of 20%-cold-worked type 316 stainless steel in EBR-II at 54 dpa is about twice that in HFIR, even though there is over 100 times more helium present in the latter case. This difference can be explained in terms of the microstructural evolution and rate-theory models for void and bubble growth.

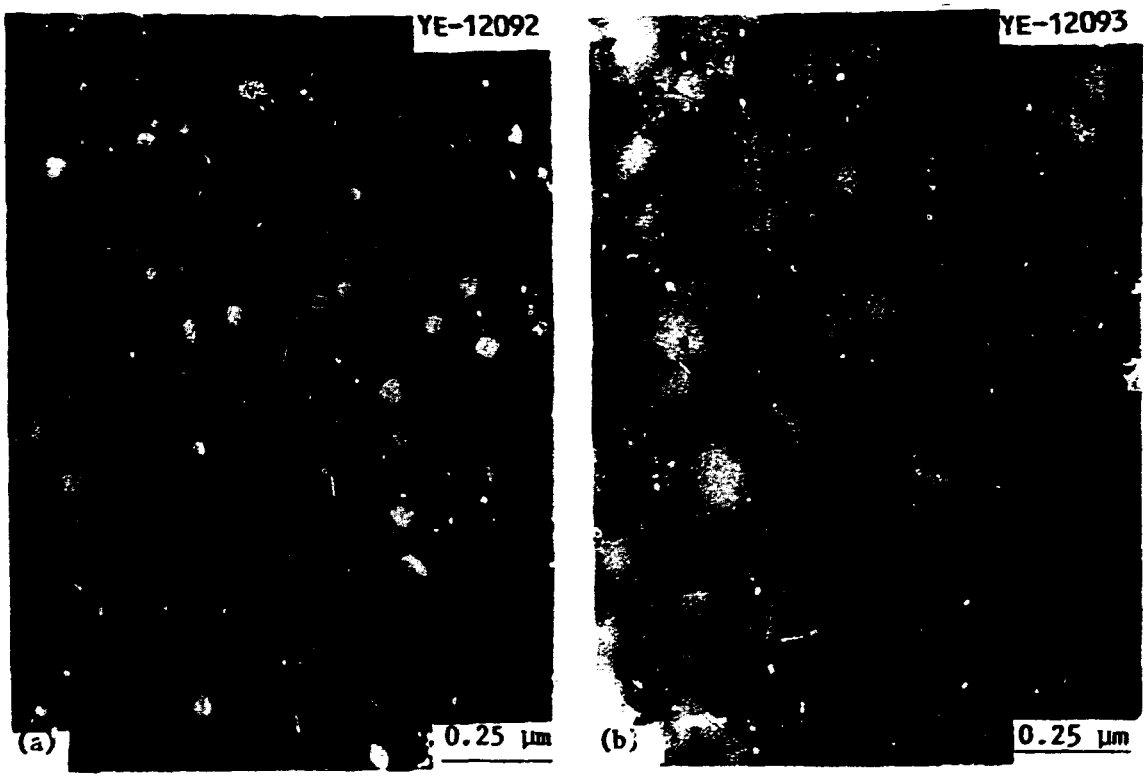

Fig. 9. Comparison of microstructures developed in 20%-cold-worked type 316 stainless steel irradiated in (a) EBR-II at 500–525°C to 8.4 dpa, ~5 at. ppm He, and (b) HFIR at 465–525°C to 11 dpa, ~600 at. ppm He (ref. [26]).

Mansur has developed the theory for cavity* growth and swelling [27] and has shown that the growth rate depends in large part on the ratio of dislocation sink strength to cavity sink strength, where that ratio $Q_{i,v}$ is given by

$$Q_{i,v} = \frac{L\, Z^d_{i,v}}{N_c\, 4\pi \bar{r}_c\, Z^c_{i,v}} \quad , \tag{4}$$

*For this discussion a cavity is the general term for either a helium bubble or a void. A bubble contains gas at or greater than equilibrium pressure, $p \geq 2\gamma/r$ (γ is the surface energy and r the bubble radius). A void contains no gas or gas at $p < 2\gamma/r$.

Fig. 10. Comparison of microstructures developed in 20%-cold-worked type 316 stainless steel irradiated in (a) EBR-II at 500–525°C to 36 dpa, ~22 at. ppm He, and (b) HFIR at 465–525°C to 54 dpa, ~3600 at. ppm He (ref. [26]).

where $Z^d_{i,v}$ is the capture efficiency of interstitials or vacancies by dislocations, L is the dislocation line density, $\bar{r}_c$ is the average cavity radius, $Z^c_{i,v}$ is the capture efficiency of interstitials or vacancies by cavities, and N_c is the cavity void density.

For $Q \gg 1$, which microstructurally coincides with a dislocation sink strength much greater than the cavity sink strength, dislocation-dominated bias-driven cavity growth occurs. (Such a condition always exists at the start of an irradiation when very few cavities are present.) Vacancies and interstitials are accepted preferentially by different sinks — interstitials by dislocations, vacancies by cavities. Under these conditions, a plot of swelling against dose (dpa) such that

$$\frac{\Delta V}{V} \propto (\text{dose})^n \qquad (5)$$

results in an n of 3/2 or 3 [27], depending on whether growth is assumed to be diffusion controlled or surface controlled, provided that dislocation density and cavity density do not change with dose, as is often the case for moderate doses in austenitic stainless steels.

When $Q \ll 1$, which coincides with a high cavity number density relative to the dislocation density, a cavity-dominated swelling mode results. The large number of cavities act as sinks for both vacancies and interstitials. Because most of the vacancies and interstitials are accepted by the same sink, the swelling rate decreases significantly, and n in Eq. (5) decreases to 3/4 or 3/5 [27]. A $Q \approx 1$ coincides with the transition from one growth mode to the other. Under these conditions the dose dependence is expected to be roughly linear.

The theory can qualitatively explain the large difference in swelling behavior at high dpa [Fig. 8(b)] as the difference between the kinetics for bias-driven (EBR-II with $Q \gg 1$) and cavity-dominated (HFIR with $Q \ll 1$) swelling modes.

It should be emphasized that the above discussion applies to 20%-cold-worked type 316 stainless steel at 500°C; a similar relative behavior has been observed at 600°C. The temperature dependence of swelling (at a given dpa) for 20%-cold-worked type 316 stainless steel is quite complicated: The temperature at which maximum swelling occurs is different in EBR-II and HFIR; thus, the curves cross over, with swelling being greater in EBR-II in certain temperature regimes and HFIR in others. Finally, the swelling relationships for solution-annealed type 316 stainless steel are still being worked out. Just as microstructural differences due to HFIR and EBR-II irradiation gave rise to differences in swelling behavior of 20%-cold-worked type 316 stainless steel, the swelling behavior of solution-annealed steel is different from that of the cold-worked material.

The above discussion illustrates the difficulties involved in interpreting results from a small data base. The initial swelling data for 20%-cold-worked type 316 stainless steel indicated much higher swelling for HFIR-irradiated material (Fig. 7). Only as more data were collected has a clearer picture developed. This discussion also illustrates how theory aids in the data interpretation. Finally, it illustrates the problems inherent in using fission reactors to obtain data applicable to fusion reactors.

The differences in swelling and precipitation caused by helium also lead to differences in the mechanical properties of stainless steels irradiated to similar dpa levels but with different helium concentrations. An example of the difference in tensile properties of irradiated steels with high and low helium concentrations is shown in Figs. 11 and 12 for solution annealed and 20%-cold-worked type 316 stainless steel. Figures 11 and 12 are taken from Bloom [7] who collected and plotted the data of various investigators. Irradiation and helium have different effects on the strengths of solution-annealed [Fig. 11(a)] and 20%-cold-worked [Fig. 12(a)] material. The most important effect of helium is noted for the ductility, where the steel with the higher helium concentrations has a significantly lower total elongation than that with less helium. This was true for both the solution-annealed [Fig. 11(b)] and cold-worked [Fig. 12(b)] material. Work is now in progress to expand the data base to a greater range of He/dpa ratios.

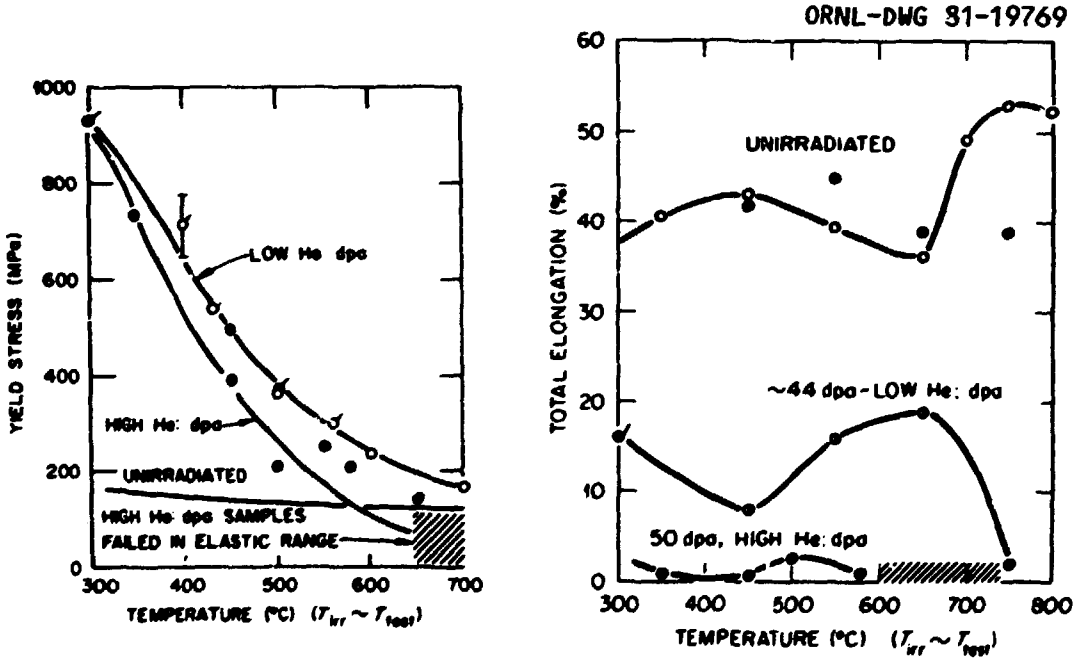

Fig. 11. Tensile properties of annealed type 316 stainless steel in the unirradiated condition and after irradiation in a fast reactor (low He/dpa) and a mixed-spectrum reactor (high He/dpa). Taken from ref. [7].

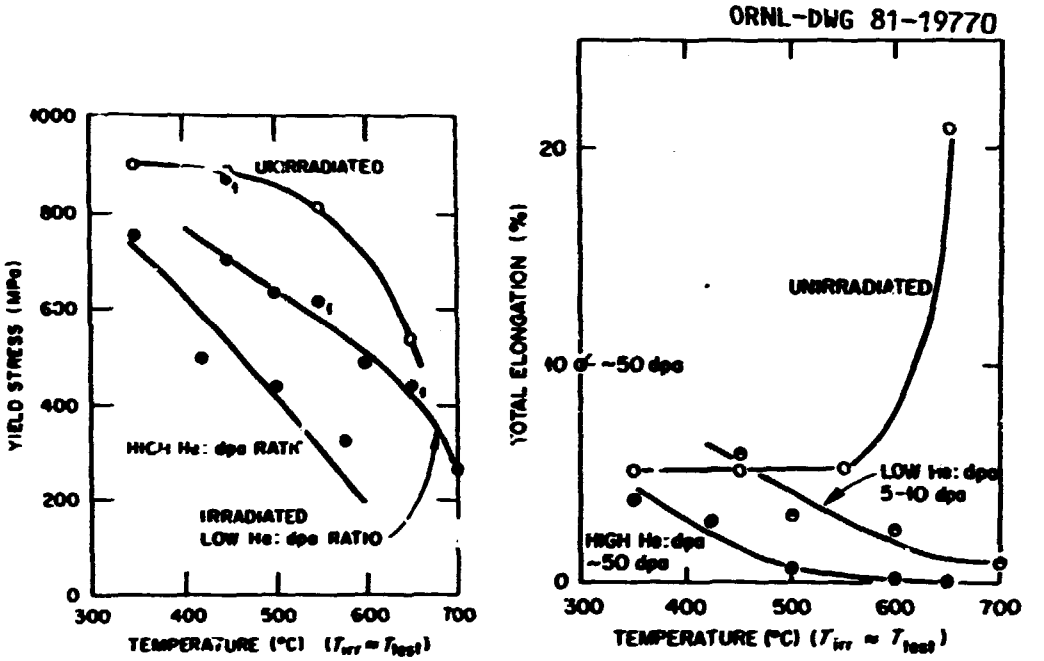

Fig. 12. Tensile properties of annealed type 316 stainless steel in the unirradiated condition and after irradiation in a fast reactor (low He/dpa) and a mixed-spectrum reactor (high He/dpa). Taken from ref. [7].

The two-step nickel-to-helium reaction can be used to study the effect of helium in any alloys containing nickel. Inconel 600 and PE-16 are the only other alloys so studied [28,29]. Qualitatively, the observed property changes were similar to those for type 316 stainless steel. Recently, the chromium-molybdenum ferritic (martensitic) steels have been included as candidates under study for first-wall and blanket structural materials [30]. Because these steels contain less than 0.5% Ni, irradiation in a mixed-spectrum reactor results in much less helium than would be formed in a fusion reactor. However, if up to 2% Ni is added to such alloys, they can be irradiated in HFIR to approximately the same He and dpa production rates as would be attained for the original unmodified alloys in a fusion reactor first-wall structure (Fig. 13). Studies are now in progress to determine the effects of helium and displacement damage on the tensile and impact properties of 9 Cr-1 MoVNb and 12 Cr-1 MoVW steels by irradiating alloys with 0, 1, and 2% Ni [31].

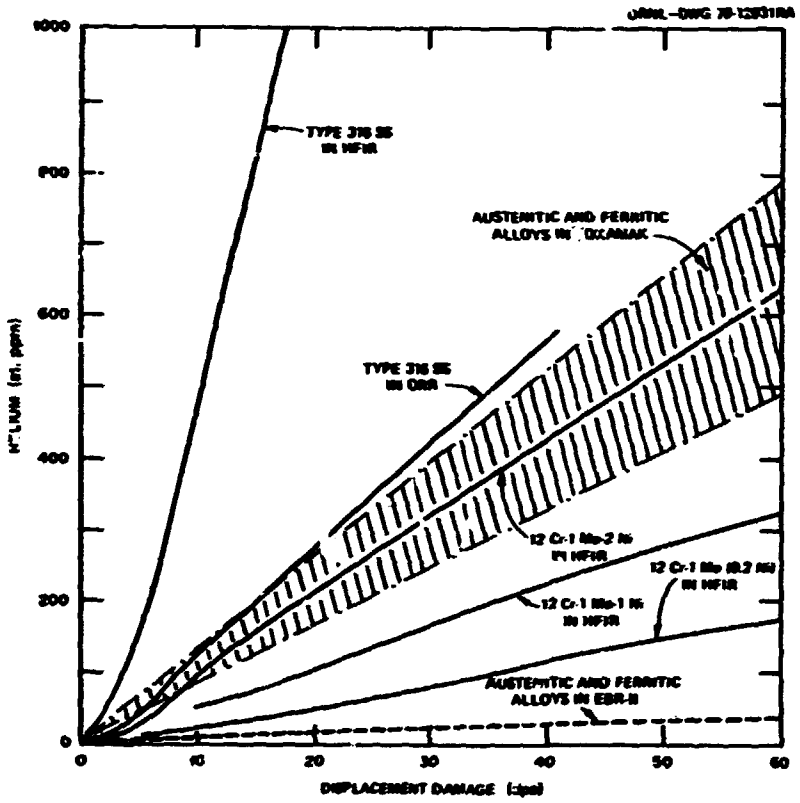

Fig. 13. Relationship between helium concentration and displacements per atom for austenitic and ferritic steels irradiated in HFIR, EBR-II, and the first wall of a fusion reactor.

For alloys of vanadium, niobium, and titanium, which are also of interest, there are no comparable methods for producing simultaneous displacement damage and transmutation gases in the alloys. Nickel generally has a limited solubility in refractory metals, and nickel additions cannot be used. The effect of displacement damage on properties can be obtained using any of the reactors discussed above. Such studies have been made and were recently reviewed [32]. At present the best technique for studying the interaction of helium with displacement damage involves the preinjection of the alloy with helium prior to irradiation in a fission reactor. This will be discussed in a later section.

3.2.4 Spectral Tailoring Experiments

The discussion in Sect. 3.2.3 shows how irradiation studies are possible under conditions where the helium is generated by transmutation of nickel by thermal neutrons. This leads to a uniform production of

helium throughout the alloy. The helium in the fusion reactor first wall and blanket structural materials is generated by transmutation reactions between most alloying elements and neutrons with energies of 6–14 MeV [19] (Fig. 2). The effect of helium in the two cases should be similar. Even for the alloys where reactions (2) and (3) apply, however, it is difficult to obtain He/dpa ratios appropriate for a fusion reactor. Such ratios can be achieved for stainless steels by "tailoring" the neutron spectrum of a mixed-spectrum reactor.

As pointed out in Sect. 3.2.2, helium concentrations and displacement damage production in type 316 stainless steel in a mixed-spectrum reactor increase at different rates. Under normal operating conditions in these reactors, this results in a one-time-only equivalence of He/dpa ratio similar to that for a fusion reactor (Fig. 6). However, it is possible to "tailor" the neutron spectrum of a mixed-spectrum reactor to closely match the ratios expected in a fusion reactor. To do this it is necessary to independently control the thermal and fast neutron fluxes. The helium production will be determined by the thermal flux, while the fast flux determines the displacement damage rate.

A hypothetical spectral tailoring experiment for the ORR is shown in Fig. 14; this calculation was made using two core positions in the reactor [33]. To change the ϕ_t/ϕ_f ratio for a given core position, several changes would have to be made in the experimental core configuration. These changes include: the number of fuel elements in the core, the mass of ^{235}U per fuel element, the thickness and species of moderators that are to be placed between the fuel and specimens, and finally, the insertion of thin pieces of aluminum that contain ~10% ^{235}U between the fuel and the test specimen [33].

In this simple proposal, no attempt was made to optimize the tailored spectrum [33]. It is not known how closely the He/dpa production must approximate that of a fusion reactor so that the same irradiation effects are obtained. In theory, it should be possible to tailor the spectrum to approach the fusion-reactor helium-dpa curve as closely as desired.

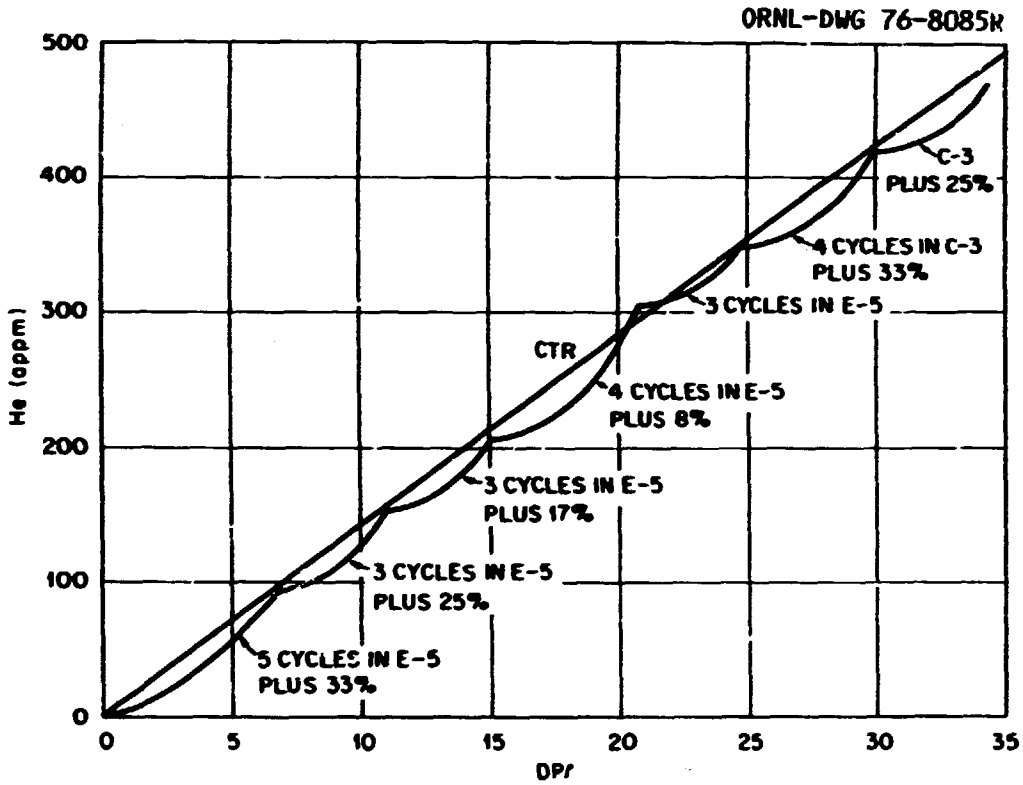

Fig. 14. Helium concentration as a function of displacements per atom in type 316 stainless steel for a fusion reactor first wall and a calculated "spectral-tailoring" experiment for the ORR. The calculation assumes two core positions, E-5 and C-3; the percentage values are for the increases in the thermal-neutron flux produced by varying the moderation between the reactor fuel and the test specimens. Taken from ref. [33].

A spectral tailoring experiment is presently in progress in the ORR (Fig. 15). [The irradiation schedule depicted in Fig. 14 was calculated for ideal conditions. Under reactor operations, various conditions (e.g., other experiments in the reactor) make it impossible to achieve such conditions.] Helium production and fast flux are monitored. With this information, detailed neutronic calculations are made to determine the time at which changes in the neutron energy spectrum should be made.

Because helium production occurs by a two-step reaction with thermal neutrons giving a concentration of helium proportional to $(\phi_t t)^n$ (n variable as discussed in Sect. 3.2.2) and dpa production is proportional

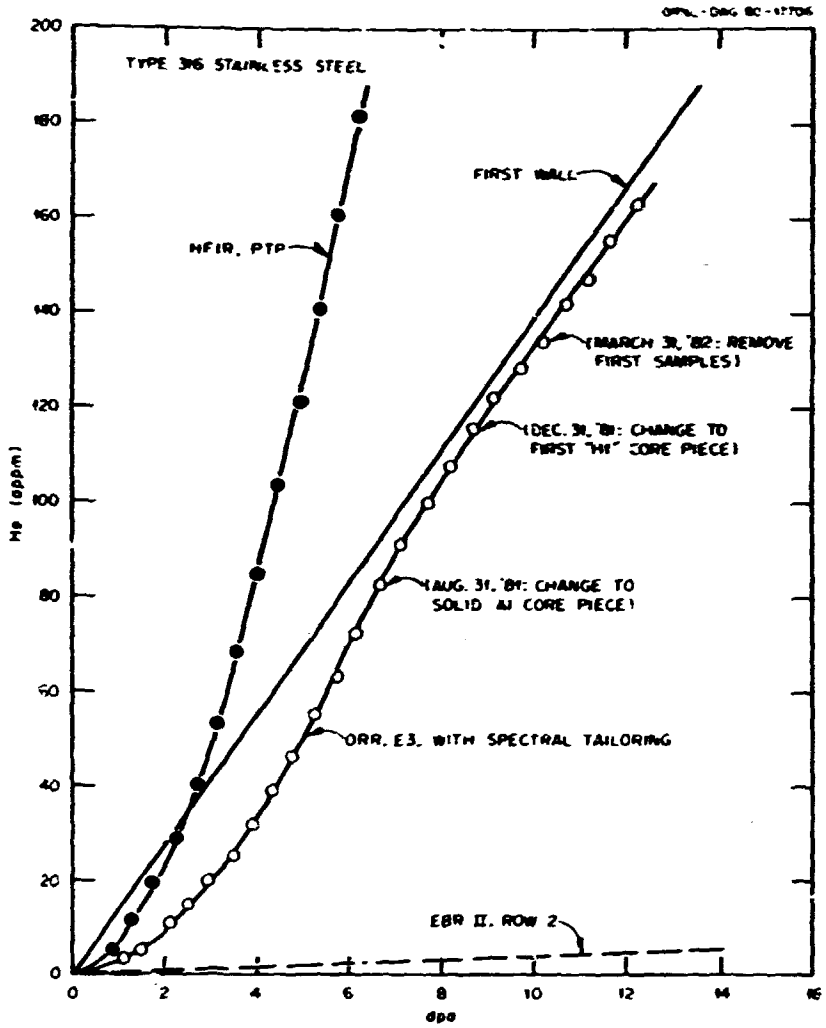

Fig. 15. Helium concentration as a function of displacements per atom in type 316 stainless steel for a spectral-tailoring experiment presently in progress in the ORR. Taken from ref. [34].

to the fast neutron fluence ($\phi_f t$), it is necessary to decrease ϕ_t or ϕ_t/ϕ_f as the experiment progresses. This is accomplished by periodic changes in the composition of the region around the experiment (e.g., water → aluminum → hafnium → hafnium + additional fuel). Details of these calculations along with an updated status of the experiment are published in periodic reports [34,35].

It is possible to envision an experiment that co ld more rapidly achieve displacement damage and helium-concentration levels appropriate for a fusion reactor. Such an experiment would use the HFIR for high helium production rates and FFTF for high displacement damage rates

(Fig. 16). Although the experimental details could present very difficult engineering problems, the potential significant advance in knowledge makes such an experiment attractive. Note that in this proposed experiment, specimens could be removed at various times in the experiment, thus making it possible to thoroughly explore the effect of helium concentration and displacement damage separately, as well as the interaction of the two.

3.3 Ion irradiation

Bombardment by high-energy ions from an ion accelerator offers another possibility for studying radiation damage for potential fusion-reactor alloys [36]. With this technique it is also possible to study the interaction

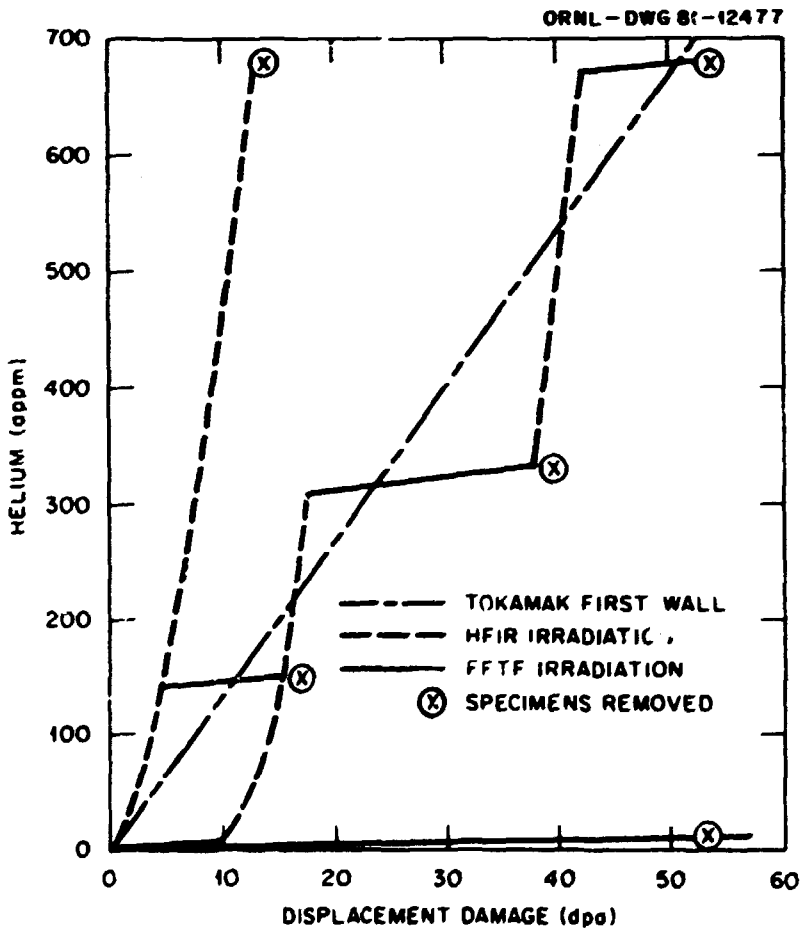

Fig. 16. Proposed "spectral-tailoring" experiment for type 316 stainless steel using the HFIR and FFTF.

of displacement damage with gases (helium and hydrogen). This can be done by either first injecting the target specimen with the gas ions followed by heavy-ion bombardment to generate the displacement damage, or the simultaneous injection of one or two gases with displacement damage (dual- or triple-beam experiments). Numerous types of ion accelerators are used for these experiments; the accelerators will not be discussed here.

The ion-beam technique has the advantages that displacement rates are much higher than those for neutron irradiations and the irradiated specimens have no residual radioactivity. This means a high damage level with high helium content can be obtained in a specimen in a short time. The dual-beam technique can be used to study the synergistic effects of helium and displacement damage on those alloys where reactors cannot be used (e.g., the refractory metal alloys). Most studies on ion-irradiated material involve transmission electron microscopy, which can be used to characterize the microstructure to determine damage mechanisms, the nature of the damage, and the extent of swelling.

Because of the differences with neutron irradiation, the technique has disadvantages. Dose equivalence is difficult or impossible to establish — that is, the swelling caused by a given dpa produced by heavy ions is considerably different from that caused by a neutron exposure to an equivalent dpa. To compare the swelling from ion bombardment with neutron irradiation, it is necessary to increase the irradiation temperature [36]. This may affect void nucleation and growth and other microprocesses. No transmutation products are formed; gases must be introduced in other ways, if these particular transmutation products are to be considered. Heavy-ion bombardment creates damage by the introduction of an extra interstitial or a foreign atom (the bombarding ion); such species could participate in the microstructural evolution. Under most irradiation conditions, the damaged region is highly localized — usually within about 1 μm from the free surface. This can give rise to an interaction between the damaged region and the surface — the surface can act as a sink for defects and permit the loss of dislocations.

Despite the above limitations, theoretical studies have shown that for pure metals and phase-stable alloys, it is possible to develop correlations between the swelling caused by heavy-ion bombardment and that caused by neutron irradiation. Much of the basic information available on the effects of transmutation-produced gases and impurities on microstructural evolution during irradiation has been obtained through bombardment experiments.

No correlations between ion bombardment and neutron irradiation are presently possible for complex multiphase alloys. Rowcliffe, Lee and Sklad compared the microstructural evolution of type 316 stainless steel during neutron irradiation and nickel-ion irradiation [37]. They found significantly different precipitation processes occurred for the different irradiation conditions. The difference existed with and without helium and led the authors to conclude that it is probably meaningless to attempt a quantitative correlation between swelling in the two environments in terms of a temperature shift and a dose equivalence factor [37].

An interesting example of an ion-bombardment study of gas effects is the work of Packan and Farrell [38]. They investigated the effect of 1400 at. ppm He and the helium-injection technique on the swelling of a single-phase austenitic alloy (Fe–17% Cr–16.7% Ni–2.5% Mo–0.005% C) irradiated to 70 dpa with 4 MeV nickel ions at 627°C. (Fig. 17). The largest amount of swelling (18%) was observed for single-ion irradiation to 70 dpa (no helium); the second largest amount of swelling (11%) was obtained for the alloy after dual-beam (helium and nickel ions) bombardment. Helium preinjection led to the lowest amount of swelling: 4 and 1% for helium preinjected at the irradiation temperature and room temperature, respectively. It was found that the final dislocation density did not depend on the helium-injection technique, although the evolution of the dislocation structure did. The change from faulted loops to dislocation networks was retarded in the specimen preinjected at room temperature [34].

The difference in swelling was explained by Packan and Farrell [38] in terms of Mansur's theoretical model [Eqs. (4) and (5)] [27]. A plot of swelling against dose revealed the differences in swelling rates for the different helium-injection techniques (Fig. 18). When the observed

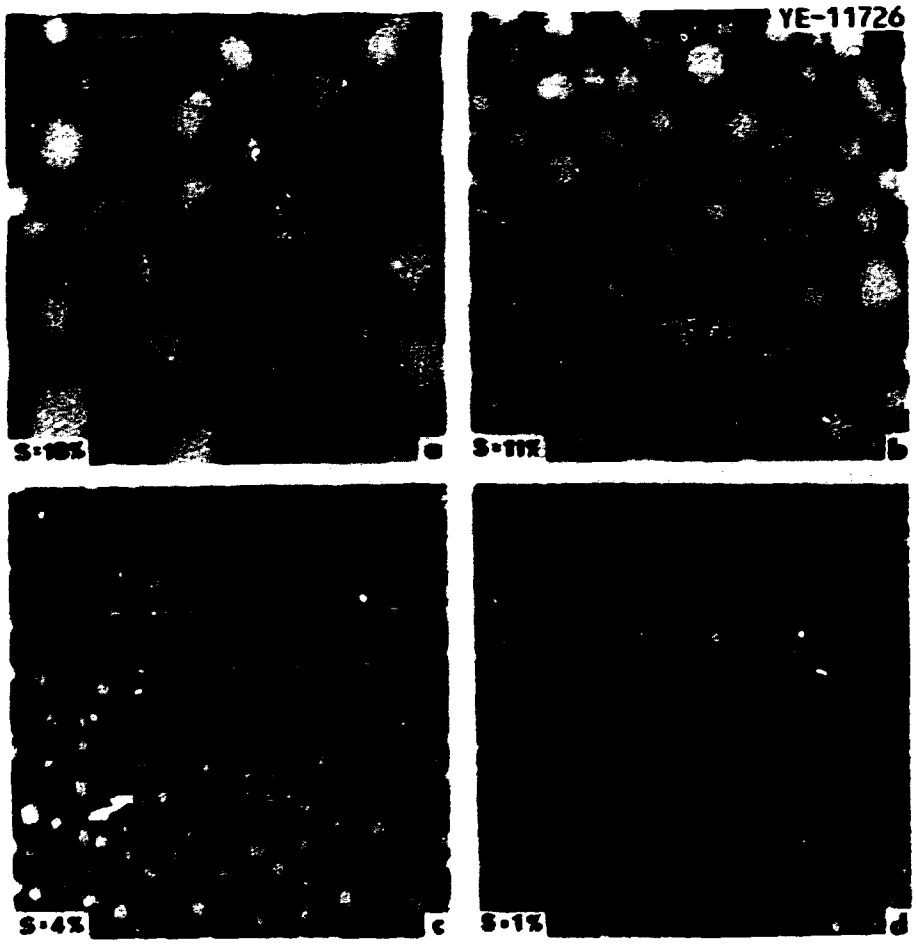

Fig. 17. Voids produced by single-ion and dual-ion bombardment of an austenitic alloy to 70 dpa at 627°C. (a) No helium added; (b) simultaneous injection of 1400 at. ppm He; (c) preinjected with 1400 at. ppm He at 627°C; (d) preinjected with 1400 at. ppm He at room temperature. Measured swelling is as shown. Taken from ref. [38].

microstructural parameters (dislocation and cavity number density) were evaluated, it was found that for room-temperature preinjection, $Q_{i,v} \ll 1$ above 10 dpa and cavities were the dominant sinks ($Q_{i,v}$ is the ratio of dislocation sink strength to cavity sink strength). For bombardments with no helium injection and simultaneous injection, voids and dislocations were found to be about equally important above about 10 dpa ($Q_{i,v} = 1$). For preinjection at 627°C, the swelling behavior between 10 and 70 dpa came to resemble that for preinjection at room temperature (i.e., a transition to $Q_{i,v} \ll 1$).

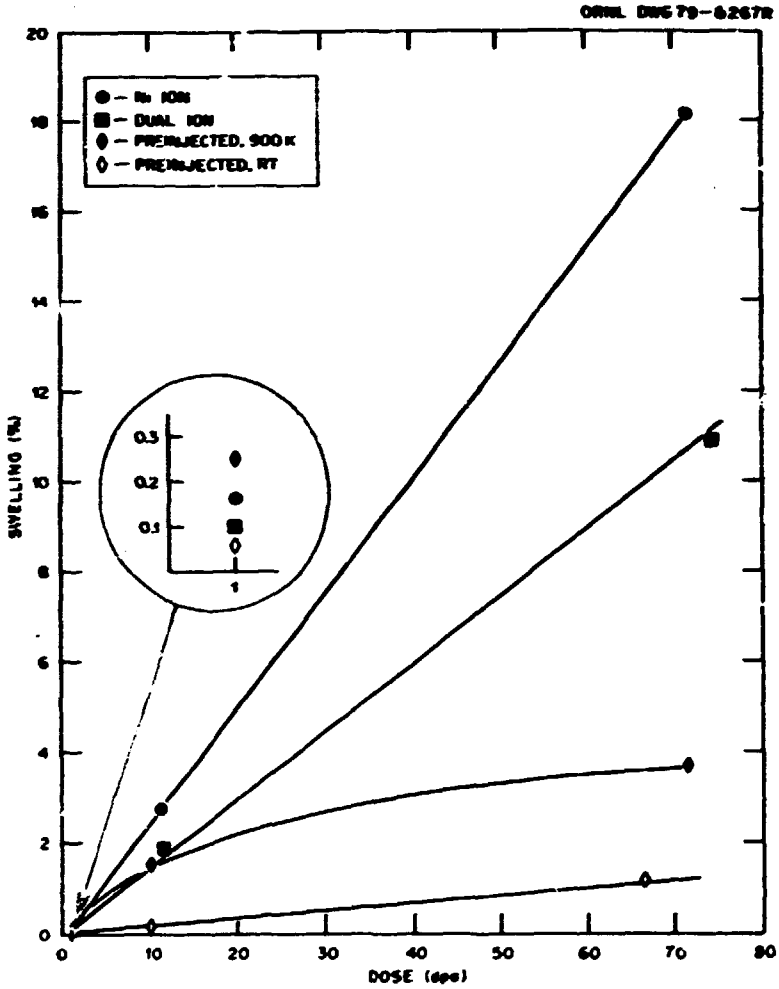

Fig. 18. Dependence of swelling on dose for different helium-injection processes. Taken from ref. [38].

Studies such as those of Packan and Farrell have been conducted on numerous materials. For example, a triple-beam irradiation technique has been used to examine the simultaneous effects of hydrogen, helium, and displacement damage on cavity formation. Hydrogen was found to have little effect [5].

Alpha-particle injection can be used to preinject specimens with helium prior to neutron irradiation, thus making it possible to achieve the desired helium and dpa levels. A uniform distribution of helium can be obtained by varying the energy of alpha particles bombarding the

specimen using a tapered energy degrader [39] and then moving the samples back and forth in front of the degraded alpha-particle beam.

This technique was recently used to preinject type 316 stainless steel, V–20% Ti, V–15% Cr–5% Ti, and Nimonic PE–16 with ~70, 90, and 200 at. ppm He at about 25°C, after which the specimens were irradiated in EBR-II. Examination by transmission electron microscopy indicated that the method used to add helium had an effect on microstructural evolution [26,40]. Cavity size and spatial distribution in type 316 stainless steel were found to be much finer in the EBR-II-irradiated preinjected specimens than those irradiated in HFIR where similar levels of transmutation helium were produced. It was also found that both the HFIR-irradiated and helium-preinjected EBR-II-irradiated cavity distributions were much finer than void distributions in uninjected EBR-II-irradiated 20%-cold-worked type 316 stainless steel at higher fluences [40]. Thus, it is again seen that helium and the method of injection are critical.

3.4 Other methods

Several other techniques have been proposed to obtain the desired He and dpa levels. One technique that is being developed is the use of stainless steel uniformly doped with ^{10}B (see, for example, ref. [41]). During irradiation of such samples by thermal neutrons, the $^{10}B(n,\alpha)^{7}Li$ reaction occurs. Unfortunately, the boron is transformed rapidly to helium. Thus, essentially all of the helium is produced in the first 10^{25} n/m^2. In essence, the technique then differs little from a preinjection technique. Furthermore, transmutation to helium is accompanied by the formation of lithium, which becomes an impurity in the host lattice and can affect the microstructural evolution.

The ^{10}B reaction was used by Gelles and Garner who analyzed helium "halos" to demonstrate the effect of helium on void formation [42]. They irradiated an austenitic stainless steel that contained 0.0007% B. Essentially all the boron was contained in small, evenly distributed precipitates that formed prior to irradiation. During irradiation in EBR-II, the boron undergoes the $^{10}B(n,\alpha)^{7}Li$ reaction. As a result the precipitates developed well-defined "atmospheres" or "halos" of helium and lithium recoil products. By analyzing the halo region high in

helium and comparing it with a region of the matrix where no helium was deposited (only displacement damage), Gelles and Garner demonstrated the importance of the simultaneous production of helium and displacement damage on cavity formation [42]. For irradiation at 400°C, they found that the swelling in the helium halo region was more than three times that of the matrix at 7×10^{26} neutrons/m^2 ($E > 0.1$ MeV). This agrees qualitatively with the comparison of HFIR and EBR-II-irradiated stainless steel [24].

A technique for obtaining helium in alloys with a high hydrogen solubility involves the "tritium trick" [43]. Tritium decays to ^{3}He with a half-life of 12 years. Thus, if the tritium is dissolved in the alloy to be tested, it will decay to ^{3}He. The amount of helium formed will depend on the alloy, the amount of tritium taken into solution (i.e., temperature of solution), and the time over which the dissolved tritium has been allowed to decay. This technique is especially useful for the refractory metal alloys, as they have quite large hydrogen solubilities [43,44]. To date the technique has been used to study the behavior of helium in metals and alloys and the effect of helium on mechanical properties [32,43,44].

In theory, the tritium trick could be used to study the effect of the simultaneous helium and displacement damage production during fission-reactor irradiations; this technique would be especially useful for niobium, vanadium, and titanium alloys which have a high solubility for hydrogen [43,44]. However, the experimental procedures involve the handling of tritium, which is difficult to contain.

Andresen and Harling [45] proposed the use of a capsule that contains ^{3}He; the ^{3}He has a high cross section for thermal neutrons for the ^{3}He(n,p)^{3}T reaction. It was proposed that the ^{3}He be contained in a pressurized capsule with the specimens to be irradiated. During irradiation in a mixed-spectrum reactor, one could obtain displacement damage from fast neutrons, while the thermal neutrons produce tritium and protium. The hydrogenic species would then be introduced into the specimens by solution or ion implantation. Beta decay then gives rise to a uniform distribution of ^{3}He in the specimens [45]. Various experimental difficulties are involved with the technique, and to date it has not been used.

4. FUTURE TEST FACILITIES

The results of the irradiation studies in the preceding sections provide valuable insight into the basic irradiation processes that will occur in fusion-reactor first-wall and blanket structural materials. With FFTF, EBR-II, and HFIR, it would be possible with long-time exposure to obtain displacement-damage levels comparable to those that will occur during the lifetime of a fusion-reactor first wall. Likewise, for alloys containing nickel, it would be possible to use HFIR and ORR to obtain helium levels comparable to those formed in a first wall. The spectral tailoring experiments offer the possibility of obtaining He/dpa ratios appropriate for a fusion reactor, but the levels do not approach those of a first wall during its lifetime. Ion-bombardment techniques could be used to rapidly produce helium and dpa levels appropriate for a fusion-reactor lifetime. However, we showed in the previous section that the interpretation of ion-bombardment results in all but pure metals and phase-stable alloys is fraught with difficulties.

Ideally, irradiation data from appropriate wall loadings would come from a demonstration fusion reactor. Such a facility is still well in the future (probably beyond the year 2000). Indeed, it would be helpful to have information on such damage levels prior to the construction of a demonstration plant. The only high-energy neutron facility presently envisioned that would allow us to begin to generate data that correlate with contemplated fusion-reactor conditions is the Fusion Materials Irradiation Test (FMIT) facility. This facility is presently planned for operation in the mid-1980s.

4.1 The fusion materials irradiation test (FMIT) facility

The FMIT is a high-energy neutron source proposed for construction in the early 1980s to be operational in approximately 1986 [46,47]. The neutrons are created by a stripping reaction caused when 35 MeV deuterons react with lithium. Figure 19 shows an overall view of the facility.

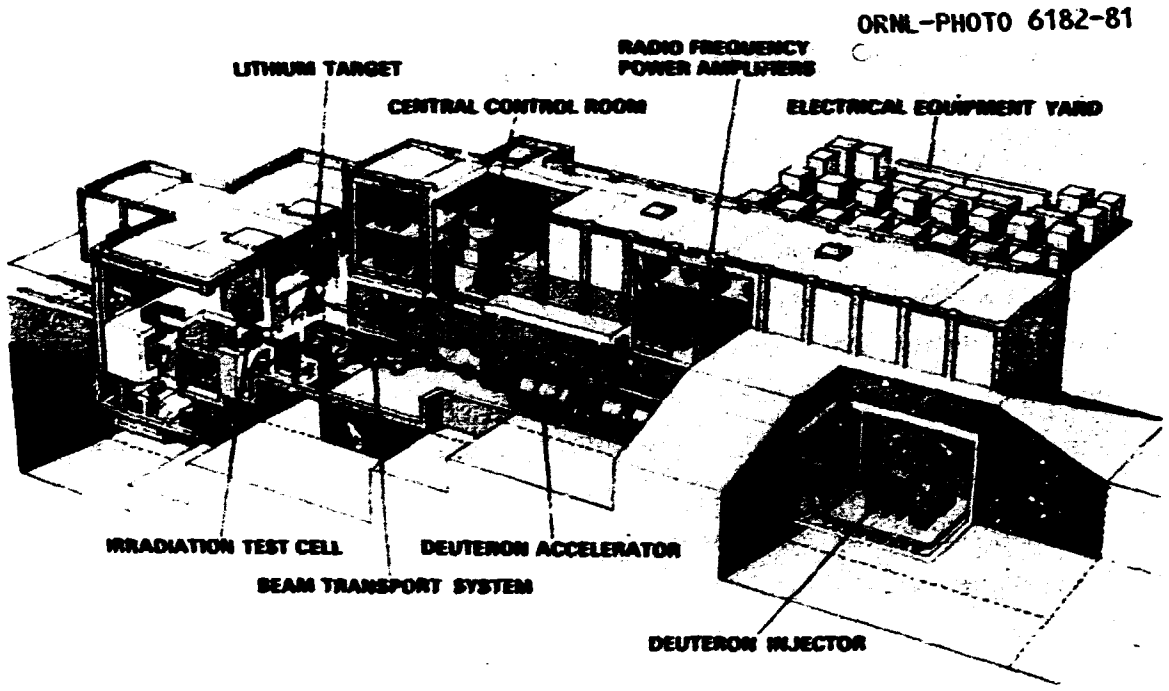

Fig. 19. Schematic diagram of the overall view of FMIT. Taken from ref. [47].

A 100 mA deuteron beam is accelerated in a LINAC. The deuteron beam is focused directly into the open face of the liquid-lithium target assembly (Fig. 20), which is essentially a "waterfall" that flows down a back target wall of stainless steel. A flow rate of about 33 liters/s is required to remove the ~3.5 MW of energy deposited in the lithium by the deuteron beam.

The 100 mA beam of 35 MeV deuterons will produce approximately 3×10^{16} neutrons/s. The neutrons are forward scattered parallel to the direction of the deuteron beam. The calculated unperturbed and perturbed neutron fluxes on the deuteron beam axis are shown in Fig. 21. The perturbed neutron flux was calculated assuming that the experimental regions (modules) were one-half the density of stainless steel. The peak flux in the experimental region nearest the target is about 4×10^{18} neutrons/$m^2 \cdot s$. Resulting displacement-damage contours and helium generation contours (using the unperturbed flux and assuming an 80% plant factor) are shown in Fig. 22. The facility will have a

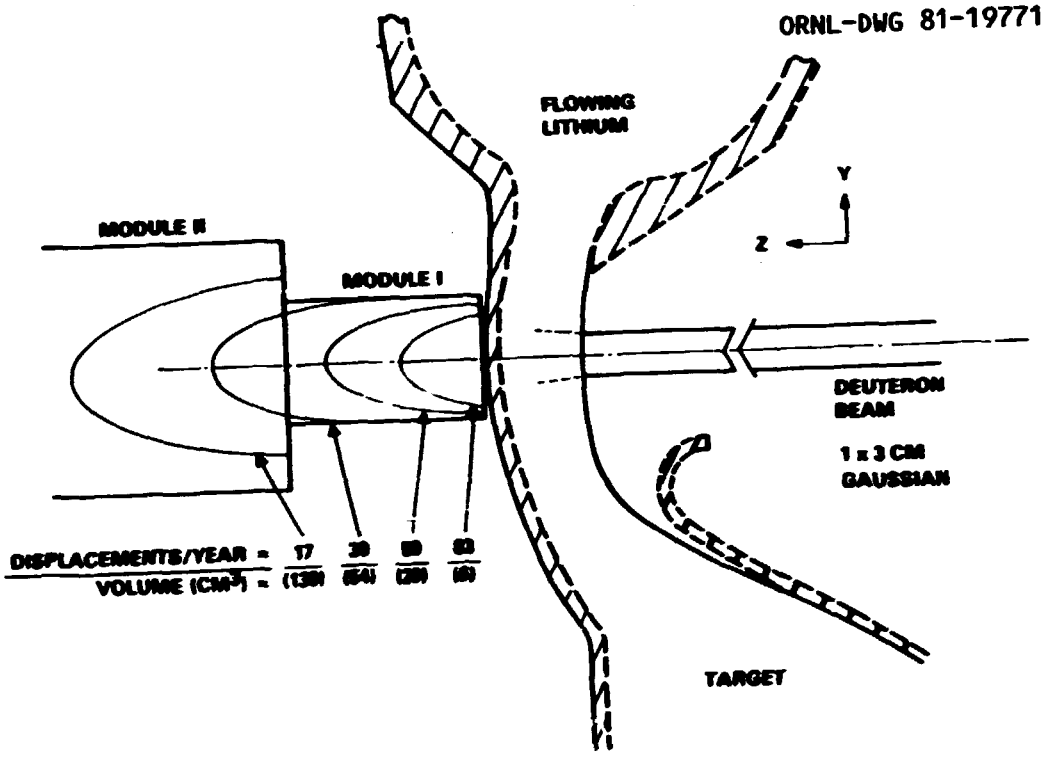

Fig. 20. Schematic diagram of deuteron beam, flowing lithium target, and test module interface and atom displacement-volume contours. Taken from ref. [47].

neutron energy spectrum which is peaked near 15 MeV with energies extending to as high as 35 MeV. It is a much closer approximation of the actual fusion spectrum than a fission reactor spectrum, and He/dpa ratios in most materials will be within a factor of 2 of those produced in the fusion spectrum.

Specimens will be irradiated in four test modules located at various distances from the target (Fig. 22). Each module will have independent temperature control. The system has a very small experimental volume: 0.139 liter within which the damage production equals or exceeds that of a fusion-reactor first wall operating at 1 MW·y/m^2. Within the test volume, large gradients in flux and spectrum exist, which preclude the irradiation of the large numbers of large samples

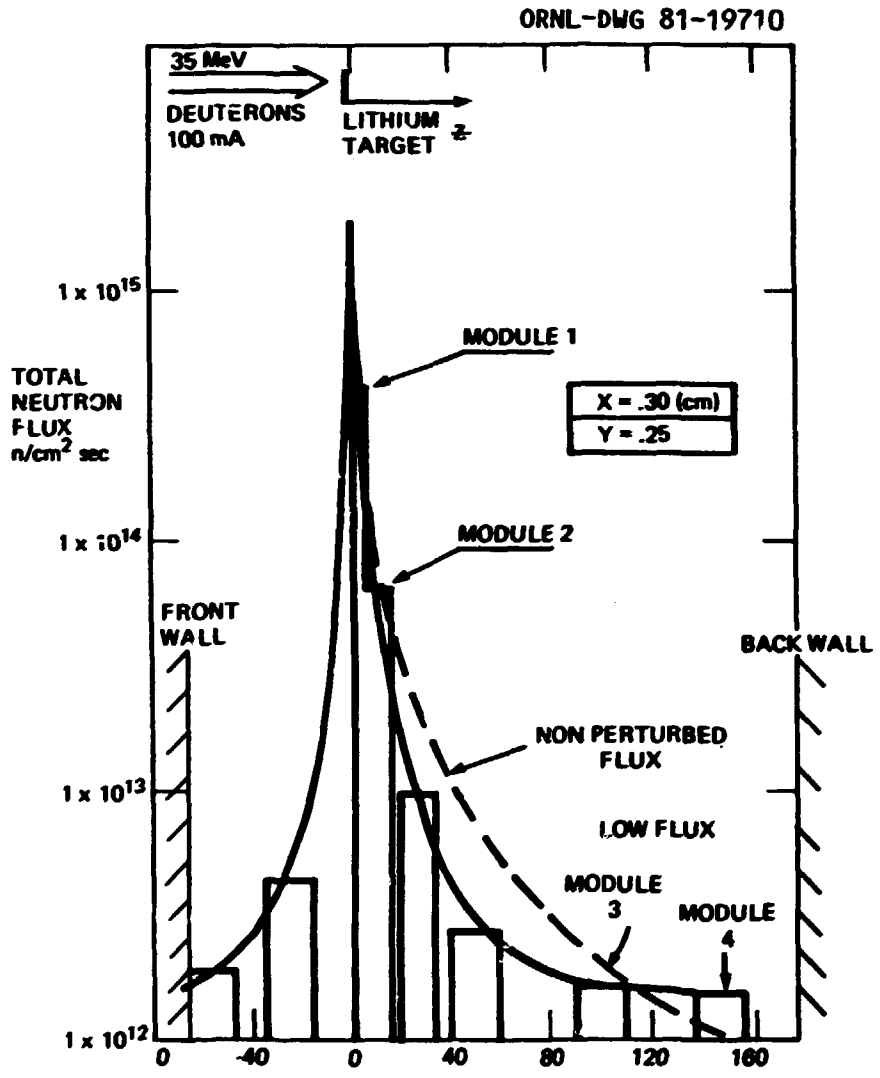

Fig. 21. Neutron flux profile along the deuteron beam center line from the front to the back of the test cell. The positions of the modules that will contain test specimens are shown. Taken from ref. [47].

required for the determination of an engineering design data base. In order to obtain maximum space utilization, miniature specimens will be used whenever possible. Examples of such miniature specimens include transmission electron microscopy disks (30-mm diameter × 3-mm thick) and 0.020- and 0.030-mm-diam tensile specimens (20-mm long). Large numbers of such specimens can be simultaneously irradiated.

The primary mission foreseen for FMIT is to develop a correlation between material response in fusion-like and fission neutron spectra.

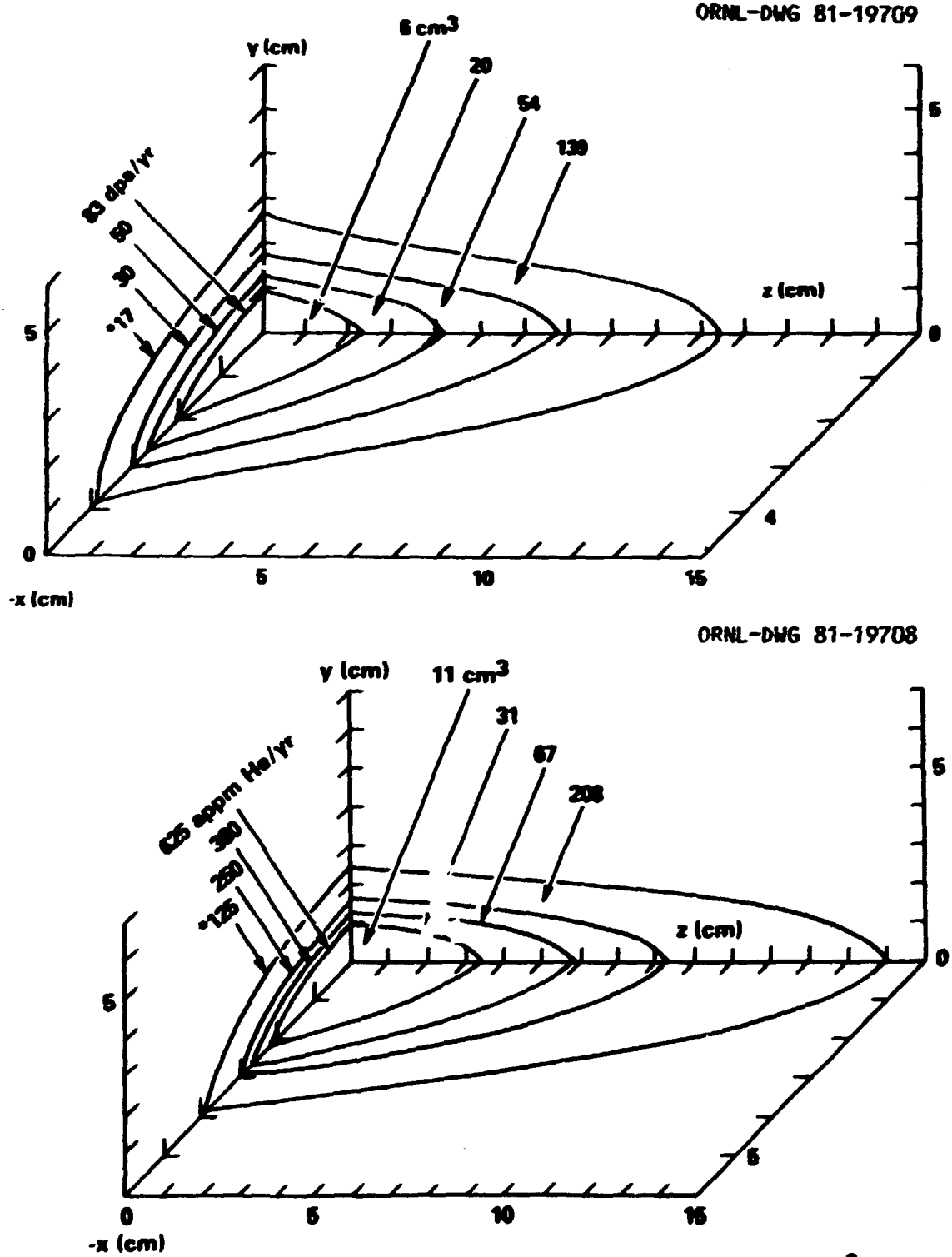

Fig. 22. (a) Displacement damage (dpa) and (b) helium concentration contours near the target (unperturbed flux). Taken from ref. [47].

These correlations will be used to predict material response in a fusion spectrum from that measured in fast- and mixed-spectrum fission reactor irradiations. In large measure, the correlations will be based on microstructural parameters and simple mechanical tests such as tensile, hardness, and irradiation creep.

5. SUMMARY

Fusion reactor first wall and blanket structural materials will experience a large neutron flux with a high-energy component unequaled in any existing neutron sources. Extended service in this neutron environment will lead to high displacement-damage levels and the formation of large amounts of helium within the structural alloys. Before a fusion reactor is built, it will be necessary to determine the effect of such an irradiation environment on the properties of the structural materials. Because no fusion reactor is presently available, the displacement damage and high-helium concentrations must be simulated using existing irradiation facilities.

Accelerator-based neutron sources (RTNS-II and d-Be sources) have been used to examine the details of damage production by high-energy neutrons. No new forms of displacement damage have been found and the amount of displacement damage created by high-energy neutrons can be calculated with reasonably good accuracy. These low-flux sources are used to establish the equivalence of the displacement damage generated by high-energy neutrons and the lower energy neutrons from fast-flux fission reactors. (Fusion neutrons are created at 14.1 MeV, while the average neutron creation energy in a fission reactor is just below 2 MeV.) Such equivalence has been demonstrated.

Fast-flux fission reactors are used to develop the high displacement damage levels that will be reached in a fusion reactor. However, this damage occurs without the high helium concentrations that are simultaneously produced in the fusion reactor. For nickel-containing alloys, large helium concentrations can be obtained by irradiation in mixed-spectrum reactors. Numerous mixed-spectrum reactor studies have

been carried out on type 316 stainless steel — a prime candidate fusion-reactor structural alloy. Such studies can also be used for the chromium-molybdenum steels if nickel is added to the base composition.

Ion bombardment studies have also helped elucidate the effect of displacement damage and high gas contents (helium or hydrogen) on the evolution of the damage microstructure. It is also possible to use ion bombardment to preinject materials with helium. Then after irradiation in a fission reactor the effect of displacement damage and helium can be determined.

By combining theoretical modeling studies with experimental irradiation studies using accelerator-based neutron sources, fission reactors, and ion bombardment facilities, we are developing a consistent picture of the processes of radiation damage and microstructural evolution that will occur in alloys in a fusion-reactor environment. The next step is the irradiation of materials to integrated neutronic wall loadings equivalent to those expected in an operating fusion reactor. One method to accomplish this for type 316 stainless steel involves the "tailoring" of the neutron spectrum in a mixed-spectrum fission reactor or by using the combined irradiations of a mixed-spectrum and fast-flux reactor. The first type of experiment is in progress.

In the mid-1980s, the FMIT facility will become available. This high-flux high-energy neutron source will allow the study of materials subjected to fluences similar to those in the first wall of an operating fusion reactor. Because of its limited test space, however, it will only provide a means of correlating the material response in fusion-like and fission neutron spectra. Until a fusion materials engineering test facility (i.e., a facility with a test volume of several liters and a fusion-reactor spectrum) is available, the materials program must rely on this combination of facilities. Each will contribute a part of the answer — none of the facilities can do the entire job by itself.

ACKNOWLEDGMENTS

We gratefully acknowledge several people who aided in this work. Detailed discussions with F. W. Wiffen and L. K. Mansur and their detailed review of the manuscript were invaluable and much appreciated.

P. J. Maziasz and N. H. Packan provided figures and information on the work depicted in the figures. The manuscript was reviewed by M. L. Grossbeck and J. O. Stiegler. The assistance of E. K. Opperman of the Hanford Engineering Development Laboratory in providing information on FMIT and obtaining permission to publish that information is appreciated. Special thanks are due Frances Scarboro for preparing several drafts and then the final copy of the report.

REFERENCES

[1] F. W. Wiffen and J. O. Stiegler, *The Technology of Controlled Nuclear Fusion*, CONF-760935-P1 (1976), p. 135.

[2] J. A. Spitznagel, F. W. Wiffen, and F. V. Nolfi, *J. Nucl. Mater.* 85&86 (1979) 629.

[3] J. T. Buswell et al., *Physical Metallurgy of Reactor Fuel Elements*, The Metals Society, London, 1975, p. 1970.

[4] J. B. Whitley, G. L. Kulcinski, and P. Wilkes, *J. Nucl. Mater.* 85&86 (1979) 701.

[5] K. Farrell, M. B. Lewis, and N. H. Packan, *Scripta Met.* 12 (1979) 112.

[6] E. E. Bloom, *Radiation Damage in Metals*, American Society for Metals, Metals Park, Ohio, 1975, p. 295.

[7] E. E. Bloom, *J. Nucl. Mater.* 85&86 (1979) 795.

[8] E. E. Bloom et al., *Proc. Third Topical Meeting on the Technology of Controlled Nuclear Fusion*, DOE CONF-780508, Vol. 1 (1978), p. 554.

[9] Lawrence Livermore Laboratory, *Rotating Target Neutron Source II Facility*, M-094 (1978).

[10] J. J. Holmes and J. L. Straalsund, *J. Nucl. Mater.* 85&86 (1979) 447.

[11] C. M. Logan, R. Booth, and R. A. Nickerson, *Nucl. Instru. & Methods*, 145 (1977) 77.

[12] J. Roberto, J. Narayan, and M. J. Saltmarsh, *Radiation Effects and Tritium Technology for Fusion Reactors*, CONF-750989 (1976), p. II-159.

[13] J. Narayan and S. M. Ohr, *J. Nucl. Mater.* 63 (1976) 454.

[14] K. L. Merkle, *Radiation Damage in Metals,* American Society for Metals, Metals Park, Ohio, 1975, p. 58.

[15] C. A. English and M. L. Jenkins, *J. Nucl. Mater.* 96 (1981) 341.

[16] J. B. Mitchell et al., *Radiation Effects and Tritium Technology for Fusion Reactors,* CONF-750989 (1976), p. II-159.

[17] R. R. Vandervoort, E. L. Raymond, and C. J. Echer, *Rad. Effects,* 45 (1980) 191.

[18] W. L. Barmore, D. W. Heikkinen, and C. M. Logan, *Magnetic Fusion Energy Quarterly Report, July-September 1979,* UCRL-50051-79-3 (February 1980), p. 41.

[19] T. A. Gabriel, B. L. Bishop, and F. W. Wiffen, *Nucl. Technol.* 38 (1978) 427.

[20] F. W. Wiffen et al., *Metals Science of Stainless Steel,* AIME New York, 1978, p. 146.

[21] R. L. Fish and J. D. Watrous, *Irradiation Effects on the Microstructure and Properties of Metals,* ASTM-STP-611, American Society for Testing and Materials, Philadelphia, 1976, p. 91.

[22] R. L. Fish and C. W. Hunter, ibid., p. 119.

[23] R. L. Fish, N. S. Cannon, and G. L. Wire, *Effects of Radiation on Structural Materials,* ASTM-STP-683, American Society for Testing and Materials, Philadelphia, 1979, p. 450.

[24] P. J. Maziasz, F. W. Wiffen, and E. E. Bloom, *Radiation Effects and Tritium Technology for Fusion Reactors,* CONF-750989 (1976) p. I-259.

[25] H. R. Brager and F. A. Garner, *Journal of Nuclear Materials,* to be published.

[26] P. J. Maziasz and M. L. Grossbeck, *Journal of Nuclear Materials,* to be published.

[27] L. K. Mansur, *Nucl. Technol.* 40 (1978) 5.

[28] F. W. Wiffen, *Effects of Radiation on Structural Materials,* ASTM-STP-683, American Society for Testing and Materials, Philadelphia, (1978), p. 88.

[29] D. N. Braski and F. W. Wiffen, *ADIP Quarterly Report, March 31, 1978,* DOE/ET-0058/1, p. 63.

[30] S. N. Rosenwasser et al., *J. Nucl. Mater.* 85&86 (1979) 177.

[31] R. L. Klueh and J. M. Vitek, to be published in *Journal of Nuclear Materials.*

[32] R. E. Gold and D. L. Harrod, *J. Nucl. Mater.* 85&86 (1979) 805.

[33] J. A. Horak and J. H. Swanks, *Trans. ANS* 26 (1977) 187.

[34] T. A. Gabriel, R. A. Lillie, and B. L. Bishop, *ADIP Quarterly Report, June 30, 1979*, DOE/ET/0058/6, p. 35.

[35] R. A. Lillie, R. L. Childs, and T. A. Gabriel, *ADIP Quarterly Report, December 31, 1980*, DOE/ER-0045/5, p. 15.

[36] K. Farrell, *Rad. Effects,* 53 (1980) 175.

[37] A. F. Rowcliffe, E. H. Lee, and P. S. Sklad, *Proceedings of Irradiation Behavior of Metallic Materials for Fast Reactor Components*, Suppl., Corse, France, p. 1.

[38] N. H. Packan and K. Farrell, *J. Nucl. Mater.* 85&86 (1979) 677.

[39] R. T. King, *Cyclotron Simulation of Neutron-Transmutation Produced Gases in Reactor Cladding and Structural Materials,* ORNL-TM-3299 (1971).

[40] P. J. Maziasz, B. L. Cox, and J. A. Horak, *ADIP Quarterly Report March 31, 1980*, DOE/ER-0045/2, p. 35.

[41] S. E. Best, A. Fadaai, and O. K. Harling, *J. Nucl. Mater.* 85&86 (1979) 835.

[42] D. S. Gelles and F. A. Garner, ibid., p. 689.

[43] W. V. Green, *Radiation Effects and Tritium Technology for Fusion Reactors,* CONF-750989 (1976), p. 372.

[44] R. F. Mattas et al., *The Technology of Controlled Nuclear Fusion,* CONF-760935-P1 (1976), p. 199.

[45] H. Andreson and O. K. Harling, *J. Nucl. Mater.* 85&86 (1979) 435.

[46] E. W. Pottmeyer, Jr., *J. Nucl. Mater.* 85&86 (1979) 463.

[47] E. K. Opperman, FMIT Experimental Capabilities, HEDL Rept. TC-1633 (1980).

ORNL-5830
Distribution
Category UC-20,20c

INTERNAL DISTRIBUTION

1–2. Central Research Library
3. Document Reference Section
4–6. Laboratory Records Department
7. Laboratory Records, ORNL RC
8. ORNL Patent Office
9. P. F. Becker
10. J. Bentley
11–15. E. E. Bloom
16. R. R. Coltman, Jr.
17. W. P. Eatherly
18. K. Farrell
19. M. L. Grossbeck
20. P. N. Haubenreich
21–23. M. R. Hill
24. J. A. Horak
25–29. R. L. Klueh
30. W. J. Lackey
31. Eal H. Lee
32. J. S. Lin
33. L. K. Mansur
34. P. J. Maziasz
35. C. J. McHargue
36. R. K. Nanstad
37. N. H. Packan
38. Y-K M. Peng
39. J. B. Roberto
40. A. F. Rowcliffe
41. M. J. Saltmarsh
42. R. T. Santoro
43. J. L. Scott
44. T. E. Shannon
45. J. Sheffield
46. D. Steiner
47. J. O. Stiegler
48. J. M. Vitek
49. J. R. Weir, Jr.
50. F. W. Wiffen
51. A. Zucker
52. A. L. Bement, Jr. (consultant)
53. E. H. Kottcamp, Jr. (consultant)
54. Alan Lawley (consultant)
55. T. B. Massalski (consultant)
56. R. H. Redwine (consultant)
57. K. M. Zwilsky (consultant)

EXTERNAL DISTRIBUTION

58–278. DOE Technical Information Center, Office of Information Services
P. O. Box 62, Oak Ridge, TN 37830

Given distribution as shown in TID-4500 under UC-20,20c

279–80. Department of Energy, Office of Fusion Energy, Washington, DC 20545

M. M. Cohen
T. C. Reuther, Jr.

281. DOE Oak Ridge Operations Office, P. O. Box E, Oak Ridge, TN 37830

Office of Assistant Manager for Energy Research and Development

282. Department of Energy, Division of Materials Sciences, Office of Basic Energy Sciences, Washington, DC 20545

L. C. Ianniello

283. Hanford Engineering Development Laboratory, P. O. Box 1970, Richland, WA 99352

E. C. Opperman

* U S GOVERNMENT PRINTING OFFICE 1981 546-067/318